Surface and Colloid Chemistry of Clays

ARTICLE *in* CHEMICAL REVIEWS · JUNE 1974

Impact Factor: 46.57 · DOI: 10.1021/cr60289a004

2 AUTHORS, INCLUDING:

Egon Matijevic
Clarkson University
536 PUBLICATIONS **16,657** CITATIONS

SEE PROFILE

1 Surface and Colloid Chemistry

K.S. Birdi

CONTENTS

1.1 INTRODUCTION TO SURFACE AND COLLOID CHEMISTRY

Matter exists as gas, liquid, and solid phases, as has been recognized by classical science. The molecules that are situated at the interfaces (e.g., between gas–liquid, gas–solid, liquid–solid, $liquid_1$–$liquid_2$, $solid_1$–$solid_2$) are known to behave differently from those in the bulk phase [1–17]. It is also well-known that the molecules situated near or at the interface (i.e., liquid–gas) are situated differently with respect to each other than the molecules in the bulk phase. Especially, in the case of complex molecules, the orientation in the surface layer will be the major determining factor as regards the surface reactions. The intramolecular forces acting would thus be different in these two cases. Furthermore, it has been pointed out that, for a dense fluid, the repulsive forces dominate the fluid structure and are of primary importance. The main effect of the repulsive forces is to provide a uniform background potential in which the molecules move as hard spheres. The attractive forces acting on each molecule in the bulk phase are isotropic when considering over an average time length. This means that the resultant net force in any direction is absent. The molecules at the interface would be under an asymmetrical force field, which gives rise to the so-called surface tension (ST) or interfacial tension (IFT) (liquid–liquid; liquid–solid; solid–solid) (Figure 1.1) [16a–c].

The resultant force on molecules will vary with time because of the movement of the molecules; the molecules at the surface will be pulled downward into the bulk phase. The presence of this force at the surface molecules will thus give rise to surface physicochemical analyses for many systems where surfaces are involved. The nearer the molecule is to the surface, the greater the magnitude of the force due to asymmetry. The region of asymmetry plays a very important role. Thus, when the surface area of a liquid is increased, some molecules must move from the interior of the continuous phase to the interface. The surface of a liquid can thus be regarded as the plane of potential energy. Analogous case would be when the solid is crushed and surface area increases per unit gram. Further, molecular phenomena at the surface separating the liquid and the

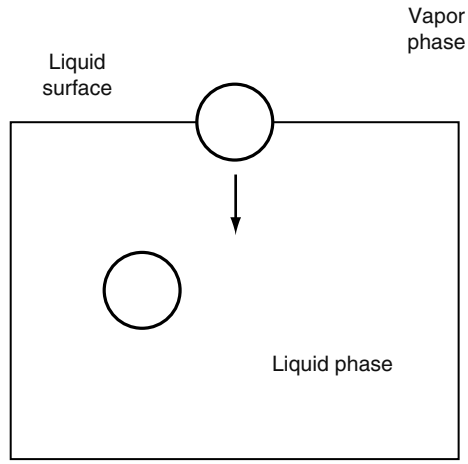

FIGURE 1.1 Intermolecular forces around a molecule in the bulk liquid and around a molecule in the surface layer (schematic).

saturated vapor are appreciably more complex than those which occur in the bulk homogeneous fluid phase. In these considerations, the gels are analyzed as under solid phase.

In the case of water, the magnitude of ST is found to decrease appreciably when some specific surface-active substances (soaps, detergents, surfactants, or amphiphiles) are added. Besides the latter property, these substances exhibit other important properties in aqueous phase. Especially, some amphiphiles exhibit the self-assembly characteristic [14]. This phenomenon is known to be the basic building block of many natural assemblies. These assemblies, also called micelles, are found to play a very important role in everyday life. The tendency of the apolar alkyl chains (hydrocarbon, HC) to be squeezed out of the aqueous medium may be considered as the driving force for micelle formation. However, the polar part of the amphiphile exhibits repulsion between the polar groups. At equilibrium between these forces, one obtains a system which corresponds to the critical micelle concentration and the aggregation number. The decrease of entropy connected with the decrease of the number of free kinetic groups is also a factor unfavorable to the micelle formation.

The microsize (nanosize) of micelles (varying in sizes of radii from 10 Å to over 1000 Å), Figure 1.2, can carry out chemical reactions both inside and at its surface, reactions which could not be possible otherwise. Micelles are actually nanoreactor systems. The most important function of micelles is their ability to solubilize organic water-insoluble substances. The role of detergents in many washing applications is well known. Further, the biological phenomena where bile salts (amphiphiles) are necessary for the solubilization and transport of lipid fats, is a very important process in the digestion. Micelle formation is an unique self-assembly property, which is found to be inherent to these amphiphile molecules [13,16,17].

The designation ''colloid'' is used for particles that are of some small dimension and cannot pass through a membrane with a pore size $\approx 10^{-6}$ m (micrometer). (Thomas Graham described this about a century ago. The Greek word for glue.). The nature and relevance of colloids is one of the main current research topics [16].

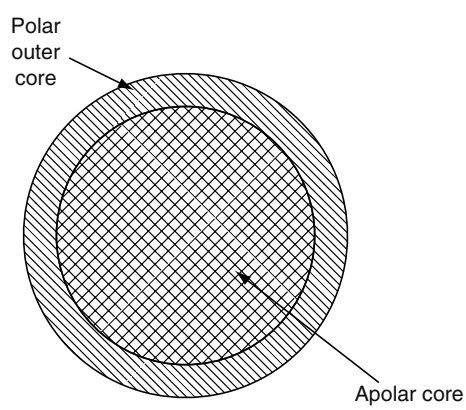

FIGURE 1.2 Micelle structure—inner core (alkane-like) and outer polar region.

The range of size determines the designation: macrocolloids to nanocolloids. Colloids are an important class of materials, intermediate between bulk and molecularly dispersed systems. The colloid particles may be spherical, but in some cases one dimension can be much larger than the other two (as in a needle-like shape). The size of particles also determines whether they can be seen with the naked eye. Colloids are neither visible to the naked eye nor under an ordinary optical microscope. The scattering of light can easily be used to see such colloidal particles (such as dust particles, etc.). The size of colloidal particles then may range from 10^{-4} to 10^{-7} cm. The units used are as follows:

$1\ \mu m = 10^{-6}$ m
1 Å (Angstrom) $= 10^{-8}$ cm $= 0.1$ nm $= 10^{-10}$ m
$1\ nm = 10^{-9}$ m

The unit Angstrom is named after the famous Swedish scientist, and currently nanometer (10^{-9} m.) unit is mainly used. Because colloidal systems consist of two or more phases and components, the interfacial area-to-volume ratio becomes very significant. Colloidal particles have a high ratio of surface area to volume compared with bulk materials. A significant proportion of the colloidal molecules lie within, or close to, the interfacial region. Hence, the interfacial region has significant control over the properties of colloids. To understand why colloidal dispersions can either be stable, or unstable, we need to consider the following:

1. Effect of the large surface area to volume ratio
2. Forces operating between the colloidal particles

If the particle size is larger than 1 μm then the system is called a suspension.

There are some very special characteristics that must be considered regarding colloidal particle behavior: size and shape, surface area, and surface charge density. The Brownian motion of the particles is a much-studied field. The fractal nature of surface roughness has recently been shown to be important [14]. Recent applications have been reported employing nanocolloids [14a]. The new innovations based on nanocolloid technology are becoming very important.

The definitions generally employed are as follows. ''Surface'' is the term used when considering the dividing phase between

Gas–liquid
Gas–solid

''Interface'' is the term used when considering the dividing phase between

Solid–liquid
$Liquid_1$–$liquid_2$
$Solid_1$–$solid_2$

In other words, the ST (γ) may be considered to arise due to a degree of unsaturation of bonds that occurs when a molecule resides at the surface and not in the bulk. However, the molecules at the surface are easily exchanging with the bulk molecules due to kinetic forces.

The term ''ST'' is used for solid–vapor or liquid–vapor interfaces. The term ''IFT'' is more generally used for the interface between two liquids, two solids, or a liquid and solid.

It is, of course, obvious that in a one-component system, the fluid is uniform from the bulk phase to the surface, but the orientation of the surface molecules will be different from those molecules in the bulk phase. For instance, one has argued that the orientation of water molecules, H_2O, at the interface most likely is consistent with the oxygen atom pointing at the interface. This would thus lead to a negative dipole and thus the rain drops would be expected to have a net negative charge (as found from experiments). The question we may ask, then, is how sharply does the density change from that of being fluid to that of gas. Is this a transition region a monolayer deep or many layers deep?

Many reports are found where this subject has been investigated [13,14]. The Gibbs adsorption theory considers surface of liquids to be monolayer. The experiments which analyze the spread monolayers are also based on one molecular layer. The subject related to self-assembly monolayer (SAM) structures will be treated extensively [14,16]. However, there exists no procedure, which can provide information by a direct measurement. This subject will be described later herein. The composition of the surface of a solution with two components or more would require additional comments [15]. In Table 1.1 are given typical colloidal suspensions that are found in everyday life. Colloidal systems are widespread in their occurrence and have biological and technological significance. There are three important types of colloidal systems [16]:

TABLE 1.1
Typical Colloidal Systems

Phases		
Dispersed	**Continuous**	**System Name**
Liquid	Gas	Aerosol fog, spray
Gas	Liquid	Foam, thin films, froth
		Fire extinguisher foam
Liquid	Liquid	Emulsion (milk)
		Mayonnaise, butter
Solid	Liquid	Sols, AgI, photography films
		Suspension wastewater
		Cement
Biocolloids		
Corpuscles	Serum	Blood
Hydroxyapatite	Collagen	Bone; teeth
Liquid	Solid	Solid emulsion (toothpaste)
Solid	Gas	Solid aerosol (dust)
Gas	Solid	Solid foam—expanded (polystyrene)
		Insulating foam
Solid	Solid	Solid suspension/solids in plastics

1. In simple colloids, clear distinction can be made between the disperse phase and the disperse medium, for example, simple emulsions of oil-in-water (o/w) or water-in-oil (w/o)
2. Multiple colloids involve the coexistence of three phases of which two are finely divided, for example, multiple emulsions of water-in-oil-in-water (w/o/w) or oil-in-water-in-oil (o/w/o)
3. Network colloids have two phases forming an interpenetrating network, for example, polymer matrix

The colloidal stability is determined by the free energy (surface free energy or the interfacial free energy) of the system.

The main parameter of interest is the large surface area exposed between the dispersed phase and the continuous phase. Since the colloid particles move about constantly, their dispersion energy is determined by the Brownian motion. The energy imparted by collisions with the surrounding molecules at temperature $T = 300$ K is $3/2\, k_B\, T = 3/2\, (1.38 \times 10^{-23})\, 300 = 10^{-20}$ J (where k_B is the Boltzmann constant). This energy and the intermolecular forces would thus determine the colloidal stability. The idea that two species should interact with one another, so that their mutual potential energy can be represented by some function of the distance between them, has been described in literature.

Furthermore, colloidal particles frequently adsorb (and even absorb) ions from their dispersing medium. Sorption that is much stronger than what would be expected from dispersion forces is called chemisorption, a process which is of both chemical and physical interest. It is thus obvious that a colloidal system represents a state of higher energy than that corresponding to the material in bulk. Hence, there will be a tendency in the system to move to lower energy state, unless there are other energetic barriers (such as electrostatic charge repulsion; steric factors; hydration forces) to overcome. Under such conditions, the system may be in a metastable state and remain in that state for a long time.

These considerations are important in regard to the different systems mentioned above: paints, cements, adhesives, photographic products, water purification, sewage disposal, emulsions, chromatography, oil recovery, paper and print industry, microelectronics, soap and detergents, catalysts, food products, pharmaceutical products, and biology (cell [adhesion and aggregation], virus).

1.2 SURFACE TENSION AND INTERFACIAL TENSION OF LIQUIDS

1.2.1 Introduction

The liquid state of matter is known to play a very important role in everyday life. The liquid surface has a very dominant role in many of these phenomena. In this context, one may mention that about 70% of the surface of earth is covered by water. The importance of rivers and rain drops on various natural phenomena is very obvious. It is therefore important to give a detailed introduction to the physicochemical principles about ST. The most fundamental characteristic of liquid surfaces is that they tend to contract to the smallest surface area to achieve the lowest free energy. Whereas gases have no definite shape or volume, completely filling a vessel of any size containing them, liquids have no definite shape but do have a definite volume, which

means that a portion of the liquid takes up the shape of that part of a vessel containing it and occupies a definite volume, the free surface being plane except for capillary effects where it is in contact with the vessel. This is observed when one notices rain drops and soap films, in addition to many other systems which will be mentioned later. The cohesion forces present in liquids and solids and the condensation of vapors to liquid state indicate the presence of much larger intermolecular forces than the gravity forces. Furthermore, the dynamics of molecules at interfaces are important in a variety of areas, such as biochemistry, electrochemistry, and chromatography.

The degree of sharpness of a liquid surface has been the subject of much discussion in the literature. There is strong evidence that the change in density from liquid to vapor (by a factor of 1000) is exceedingly abrupt, that is, in terms of molecular dimensions. The surface of a liquid was analyzed by light reflectance investigations, as described by Fresnel's law. Various investigators indeed found that the surface transition involves just one layer of molecules. In other words, when one mentions surfaces and investigations related to this part of a system, one actually mentions just a molecular layer. However, there exists one system which clearly shows the ''one molecule thick'' layer of surface as being the surface of a liquid: this is the monolayer studies of lipids spread on water and studied by Langmuir balance [18]. The surface thermodynamics of these monolayers is based on unimolecular layer at the interface, which thus confirms the thickness of the surface. The molecules of a liquid in the bulk phase are in a state of constant unordered motion like those of a gas, but they collide with one another much more frequently owing to the greater number of them in a given volume (as shown here):

Gas phase (molecules in gas)
Intermediate phase
Liquid surface (surface molecules)
Bulk liquid phase (molecules inside liquid)

It is important to notice that the intermediate phase is only present between the gas phase and the liquid phase. Although one does not often think about how any interface behaves at equilibrium, the liquid surface demands special comment. The surface of a liquid is under constant agitation; there are few things in nature presenting an appearance of more complete repose than a liquid surface at rest. On the other hand, the kinetic theory tells us that molecules are subject to much agitation. This is apparent if we consider the number of molecules which must evaporate each second from the surface to maintain the vapor pressure. At equilibrium, the number of liquid molecules that evaporate into the gas phase is equal to the number of gas molecules that condense at the liquid surface (which will take place in the intermediate phase). The number of molecules hitting the liquid surface is considered to condense irreversibly [16a]. From the kinetic theory of gases, this number can be estimated as follows:

$$\begin{aligned} \text{mass/cm}^2\text{/s} &= \rho_{\text{G}} \left(\frac{k_{\text{B}} T}{2\pi m_{\text{m}}} \right)^{0.5} \\ &= 0.0583\ p_{\text{vap}} (M_{\text{w}}/T) \end{aligned} \tag{1.1}$$

where
k_{B} is the Boltzmann constant (1.3805×10^{-16} erg deg^{-1})
m_{m} is the mass of molecule
ρ_{G} is the density of the gas
M_{w} is the molecular weight

If we consider water at 20°C, the vapor pressure of this liquid is 17.5 mm, which gives 0.25 g/s/cm^2 from Equation 1.1. This corresponds to 9×10^{21} molecules of water per second. While from consideration of the size of each water molecule, we find that there are $\approx 10^{15}$ molecules, so that it can be concluded that the average life of each molecule in the surface is only about one eight-millionth of a second ($1/8 \times 10^{-6}$ s). This must be compounded with the movement of the bulk water molecules toward the surface region. It thus becomes evident that there is an extremely violent agitation in the liquid surface. In fact, this turbulence may be considered analogous to the movement of the molecules in the gas phase. One observes this vividly in a cognac glass. In the case of interface between two immiscible liquids due to the presence of IFT, the interface tends to contract. The magnitude of IFT is always lower than the ST of the liquid with the higher tension. The liquid–liquid interface has been investigated by specular reflection of x-rays to gain structural information at Angstrom (Å $= 10^{-8}$ cm $= 0.10$ nm) resolution [19–21].

The term ''capillarity'' originates from the Latin word capillus, a hair, describing the rise of liquids in fine glass tubes. Laplace showed that the rise of fluids in a narrow capillary was related to the difference in pressure across the interface and the ST of the fluid [22–24]:

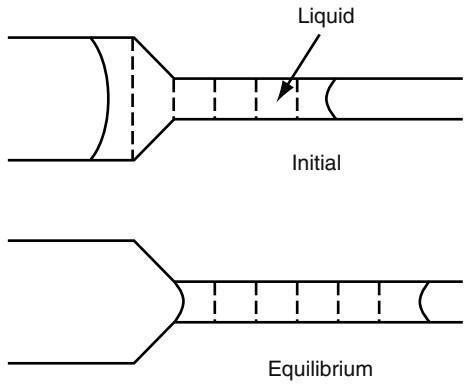

FIGURE 1.3 Capillary flow of liquid due to Laplace pressure.

$$\begin{aligned}\Delta P &= \gamma(\text{curvature}) = \gamma\left(\frac{1}{\text{radius of the curvature}}\right)\\ &= 2\gamma\left(\frac{1}{\text{radius of the capillary}}\right)\end{aligned} \tag{1.2}$$

This means that when a glass tube of a hair-fine diameter is dipped in water, the liquid meniscus will rise to the very same height. A fluid will rise in the capillary if it wets the surface, whereas it will decrease in height if it nonwets (like Hg in glass capillary). The magnitude of rise is rather large, that is, 3 cm if the bore is of 1 mm for water. This equation also explains what happens when liquid drops are formed at a faucet. Although it may not be obvious here, but the capillary force can be very dominating in different processes. In Figure 1.3, it is found that the flow of liquid takes place due to the ΔP only, since there is practically no gravity force present. In porous materials, this capillary force thus becomes the most significant driving force.

The same is found in the case of two bubbles or drops, Figure 1.4, where the smaller bubble or drop (due to lager ΔP) will coalescent with the larger bubble or drop.

The capillary phenomenon thus means that it will play an important role in all kinds of systems where liquid is in contact with materials with pores or holes. In such systems the capillary forces will determine the characteristics of liquid–solid systems. Some of the most important are:

- All kinds of fluid flow inside solid matrices (ground water; oil recovery)
- Fluid flow inside capillary (oil recovery; ground water flow; blood flow)

It was recognized at a very early stage that only the forces from the molecules in the surface layer act on the capillary rise. The flow of blood in all living species is dependent on the capillary forces. The oil recovery technology in reservoirs is similarly dependent on the capillary phenomena. Actually, the capillary forces become very dominating in such systems. Furthermore, virtually all elements and chemical compounds have a solid, liquid, and vapor phase. A transition from one phase to another phase is accompanied by a change in temperature, pressure, density, or volume. This observation thus also suggests that due to the term ΔP, the chemical potential will be different than in systems with flat surfaces. In a recent study, the cascade of a structure in a drop falling from a faucet was investigated [25]. In fact, fluid in the shape of drops (as in rain, sprays, fog, emulsions) is a common natural phenomenon and has attracted the attention of scientists for many decades.

A molecular explanation can be useful to consider in regard to surface molecules. Molecules are small objects which behave as if of definite size and shape in all states of matter (e.g., gas [G], liquid [L], and solid [S]) [26]. The volume occupied by a molecule in the gas phase is some 1000 times larger than the volume occupied by a molecule in the liquid phase, as follows:

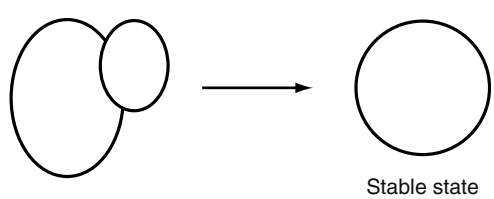

FIGURE 1.4 Smaller drop (or bubble) will merge into the larger drop due to the difference in the Laplace pressure.

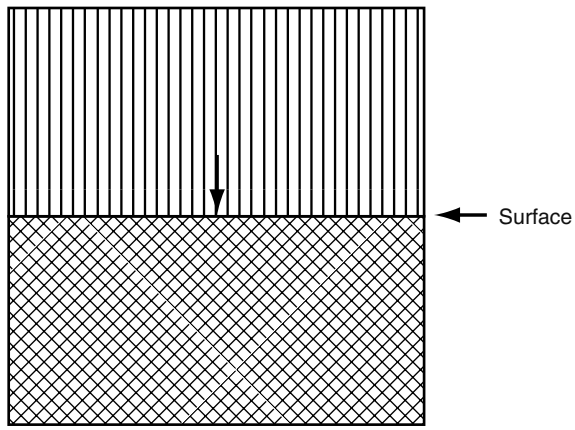

FIGURE 1.5 Tension in liquid surface.

As shown above, the volume of 1 mol of a substance—for example, water in the gas phase (at standard temperature and pressure), V_G (≈24,000 cc/mol)—is some 1000 times its volume in the liquid phase, V_L (molar volume of water ≈18 cc/mol). The distance between molecules, D, will be proportional to $V^{1/3}$ such that the distance in the gas phase, D_G, will be approximately 10 ($1000^{1/3}$) times larger than in the liquid phase, D_L. The finite compressibility and the relatively high density, which characterize liquids in general, point to the existence of repulsive and attractive intermolecular forces. The same forces that are known to be present in the gaseous form of a substance may be imagined to play a role also in the liquid form. The mean speed of the molecules in the liquid is the same as that of the molecules in the gas; at the same temperature, the liquid and gas phase differ mainly by the difference in the density between them.

The magnitude of ST, γ, is determined by the internal forces in the liquid, thus it will be related to the internal energy or cohesive energy. The ST or capillary phenomena was mentioned in the literature at a very early stage by Leonardo da Vinci [27,28].

The phenomena of ST can be explained by assuming that the surface behaves like a stretched membrane, with a force of tension acting in the surface at right angles, which tends to pull the liquid surface away from this line in both directions (Figure 1.5).

ST thus has units of force/length = mass × distance/time^2 distance = mass/time^2. This gives ST in units as mN/m or dyn/cm or J/m^2 (mN m/m^2). As another example, one can imagine a rectangular frame with a sliding wire, EF, fitted with a scale pan (Figure 1.6). If the frame is dipped into a soap (or any detergent) solution, a surface film (denoted as EBCF) will be formed. The ST would give rise to a tendency for the film to contract, to achieve a minimum in free energy. The weight, w_f, thus required to balance this force would be

$$w_f = 2\gamma\ [EF] \tag{1.3}$$

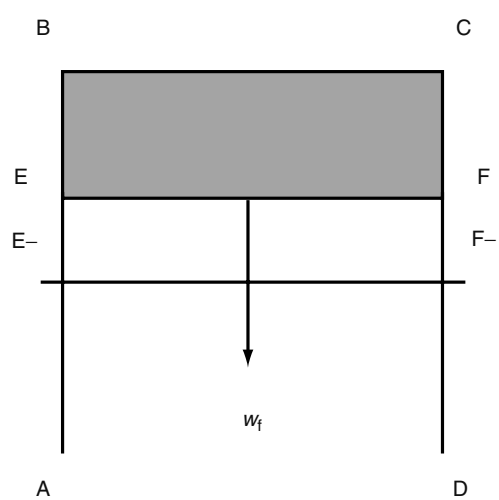

FIGURE 1.6 Stretching of a thin liquid film.

Volume per Mole in Gas or Liquid Phase and Distance between Molecules in Gas and Liquid Phases

Molar volume of water (at 20°C)
V_{gas} = ca. 24,000 mL (as gas)
V_{liquid} = ca. 18 mL (as liquid)
Ratio
V_{gas}: V_{Liquid} = ca. 1000
Distance (D) between molecules in gas (D_G) or liquid (D_L) phase
Ratio D_G: $D_L = (V_G: V_L)^{1/3} = (1000)^{1/3} = 10$

The factor 2 in Equation 1.3 arises from the two sides of the film. If the film is stretched to a new EBCF point, the work done on the system is

$$\begin{aligned} \text{Work} &= w_f\ [EE'] \\ &= 2\gamma\ [EF.EE'] \\ &= 2\gamma\ [E'EFF'] \\ &= 2\gamma\ (\text{increase in area}) \end{aligned} \tag{1.4}$$

Gibbs [29] defined ST as the free energy excess per unit area:

$$\begin{aligned} \gamma &= \frac{G - (G^a - G^b)}{\text{Area}} \\ &= \frac{G_{surface}}{\text{Area}} \end{aligned} \tag{1.5}$$

where G is the free energy of the two-phase system (phases a and b). The liquid and vapor phases are separated by a surface region [2,5,7,13,14,28–34].

It is also seen that other thermodynamic quantities would be given as [16]

$$\text{Surface energy} = U_{surface} = \frac{U}{\text{Area}} \tag{1.5a}$$

$$\text{Surface entropy} = S_{surface} = \frac{S}{\text{Area}} \tag{1.5b}$$

and from this one can obtain

$$\gamma = U_{surface} - S_{surface} \tag{1.5c}$$

Hence, the magnitude of ST is also equal to the work spent in forming unit surface area (m^2 or cm^2). This work increases the potential energy or free surface energy, G_s ($J/m^2 = erg/cm^2$) of the system. This can be further explained by different observations one makes in everyday life, where liquid drops contract to attain minimum surfaces. If a loop of silk thread is laid carefully on a soap film and the inside the loop is pricked with a needle, the loop takes up a circular shape, which provides a minimum in the energy for the system (Figure 1.7). Indeed, the concept of ST was already accepted around the year 1800. The

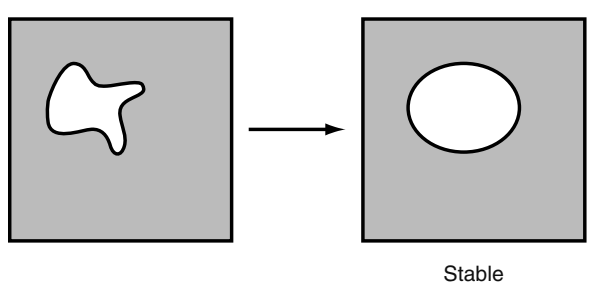

FIGURE 1.7 ST causes the equilibrium in the right drawing, where a circular shape is present.

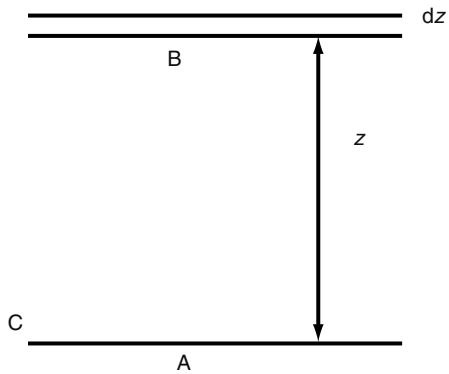

FIGURE 1.8 Pressure gradient in the surface region. (A and B are two parts of fluid divided by plane C; dz is an imaginary thin layer in z-axis.) (Schematic)

observations such as a floating metal pin on the surface of water have been a common experience to all youngsters. In fact, a great many aquatic insects survive by floating on the surface of water in lakes due to surface forces.

It is well-known that the attraction between two portions of a fluid decreases very rapidly with the distance and may be taken as zero when this distance exceeds a limiting value, R_c, the so-called range of molecular action. According to Laplace [1,4,35,36], ST, γ, is a force acting tangentially to the interfacial area, which equals the integral of the difference between the external pressure, p_{ex}, and the tangential pressure, p_t:

$$\gamma = \int (p_{ex} - p_t)\, dz \tag{1.6}$$

The z-axis is normal to the plane interface and goes from the liquid to the gas (Figure 1.8). The magnitude of work which must be used to remove a unit area of a liquid film of thickness t will be proportional to the tensile strength (latent heat of evaporation) of the liquid thickness. In the case of water, this would give approximately 25,000 atm of pressure (600 cal/g = ca. 25.2×10^9 erg = 25,000 atm). However, different theoretical procedures used to estimate γ by using Equation 1.6 have been subject to much difficulty, some of these procedures have been analyzed in a review [37]. In this review, the energetics and hydrostatic forces were analyzed. The change in density which occurs near the interface was also discussed. Further, due to the asymmetry of surface force fields as mentioned herein, the outermost layer of surface molecules in a liquid will be expected to be highly structured, for example, in the case of water, leading to well-defined structural orientations such as polychair or polyboat surface networks [38,39]. In the same way, ST can be described by quantitative structure–activity relationship (QSAR) or the so-called parachor (as described briefly in Section 1.2.2). QSAR is an analysis by which the molecular structure of a series of molecules is correlated to its major characteristics. It has been known for long time that QSAR approach can be applied to small molecule series, such as benzene, toluene, ethyl-benzene, etc.

1.2.2 Parachor (or Quantitative Structure–Activity Relationship)

In all kinds of technology, it is most useful to be able to predict physical property of a molecule from some theoretical criteria. Especially, it is important that one can correlate some molecular property to its structure (both quantitative and qualitative). In current literature, one finds extensive analyses of QSAR as applied to different systems. Many physical properties of molecules in the bulk phase can be related to their composition and structure [40]. This is very convenient when one needs to be able to predict the properties of any molecule and also from a theoretical viewpoint, which gives one a more molecular understanding of the different forces present in any system. At a very early stage, it was accepted that the same could be expressed for the ST and bulk characteristics. The most significant observation was that the expression relating ST with density (ρ_L and ρ_G: for liquid and gas) was independent of temperature:

$$\frac{\gamma^{1/4}}{(\rho_L - \rho_G)} = C_{para} \tag{1.7}$$

The above equation was useful in the determination of molecular properties [41]. After multiplication of both sides by the molecular weight, M_w, the constant, C_{para}, is called the parachor (P_{para}):

$$P_{para} = C_{para}\, M_w = \frac{M_w \gamma^{1/4}}{(\rho_L - \rho_G)} \tag{1.8}$$

TABLE 1.2
QSAR for Estimating the Parachor Values

Parachor Values									
C	H	O	F	Cl	Br	I	N	S	P
4.8	17.1	20	25.7	54.3	68	91	12.5	48.2	38.2
Parachor Values									
CH_3	CH_2	C_6H_5	COO	COOH	OH	NH_2	NO_2	NO_3	$CONH_2$
56	40	190	64	74	30	43	74	93	92

Sources: From Birdi, K.S., ed., *Handbook of Surface & Colloid Chemistry*, CRC Press, Boca Raton, FL, 1997; Birdi, K.S., ed., *Handbook of Surface & Colloid Chemistry-CD Rom*, CRC Press, Boca Raton, FL, 1997; *Handbook of Surface & Colloid Chemistry*, 2nd edn., 2002.

The parachor quantity, P_{para}, is primarily an additive term such that each group of molecules contributes to the same extent in a homologous series. If one neglects ρ_G in comparison to ρ_L (an error of less than 0.1%), then we get

$$P_{\text{para}} = M_w \gamma^{1/4} \frac{\rho}{p_L} = V_m \gamma^{1/4} \tag{1.9}$$

where V_m is the molar volume of the liquid. The adaptivity of parachors is thus equivalent to that of atomic volumes measured under unit ST, which is regarded to be approximately the same as under equal internal pressures.

The atomic and constitutional parachor values are given in Table 1.2. Furthermore, the parachor values for single bond (sb); coordinate bond (cb); double bond (db); triple bond (tb); single-electron bond (seb); 3-, 4-, 5-, 6-, 7-, or 8-membered rings (3r, etc.); and a naphthalene ring (na) were given as follows [40–43]:

Parachor Values											
Seb	**sb**	**cb**	**db**	**tb**	**3r**	**4r**	**5r**	**6r**	**7r**	**8r**	**na**
−11.6	0	−1.6	23.2	46.6	16.7	11.6	8.5	6.1	4.6	2.4	12.2

As an example, the calculated value for tolunitrile, $C_6H_4CH_3CN$, is found as

$$8 \times 4.8 + 7 \times 17.1 + 1 \times 12.5 + 46.6 + 3 \times 23.2 + 6.1 = 292.9$$

The measured values of parachor are 290.6, 295.5, and 294.4 for the ortho, meta, and compound, respectively. The calculated values for some typical liquids agreed satisfactorily with the measured data (inside brackets):

Acetone: 23.35 (23.09)
Ethanol: 21.92 (22.03)
n-octane: 21.3 (21.32)

Parachors in solutions can also be estimated, but it has been reported to be more difficult. This arises from the fact that the composition of the surface is different from that of the bulk phase. The present state of analysis is not very satisfactory [40–44]. Furthermore, the parachor theory for IFT remains to be investigated; therefore, some suggestions will be developed in this review. However, some typical data are found in literature where ST for various mixed systems is given along with density, refractive index, and viscosity [45a–j]:

- Density and ST of aqueous H_2SO_4 at low temperature [45b–j]
- Density, viscosity, and ST of sodium carbonate + sodium bicarbonate buffer solutions in the presence of glycerin, glucose, and sucrose from 25°C to 40°C [45b–j]
- Density, ST, and refractive index of aqueous ammonium oxalate solutions from 293 to 333 K [45b–j]
- STs, refractive indexes, and excess molar volumes of hexane + 1-alkanol mixtures at 298.15 K [45b–j]
- Densities, viscosities, refractive indices, and STs of 4-methyl-2-pentanone + ethyl benzoate mixtures at 283.15, 293.15, and 303.15 K, respectively [45b–j]

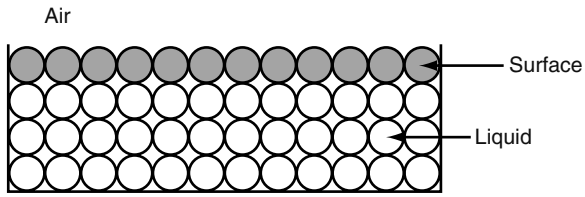

FIGURE 1.9 Molecular packing in two dimensions in bulk (six near neighbors) and surface (three near neighbors) molecules (schematic).

1.2.3 Heat of Surface Formation and Heat of Evaporation

All natural phenomena are dependent on temperature and pressure. As mentioned earlier, energy is required to bring a molecule from the bulk phase to the surface phase of a liquid. In the bulk phase, the number of neighbors (six near neighbors for hexagonal packing and if considering only two-dimensional packing) will be roughly twice the molecules at the surface (three near neighbors, when discounting the gas-phase molecules) (see Figure 1.9).

The interaction between the surface molecules and the gas molecules will be negligible, since the distance between molecules in the two phases will be very large. Furthermore, as explained elsewhere, these interaction differences disappear at the critical temperature. It was argued [7,46] that when a molecule is brought to the surface of a liquid from the bulk phase (where each molecule is symmetrically situated with respect to each other), the work done against the attractive force near the surface will be expected to be related to the work spent when it escapes into the vapor phase. It can be shown that this is just half for the vaporization process (Figure 1.9).

The density, viscosity, and ST of liquid quinoline, naphthalene, biphenyl, decafluorobiphenyl, and 1,2-diphenylbenzene from 300°C to 400°C, have been reported [47].

In earlier literature, several attempts were made to find a correlation between the latent heat of evaporation, L_{evap}, and γ or the specific cohesion, $a_{co}^2(2\gamma/\rho_L = 2\gamma v_{sp})$, where $\rho_L =$ density of the fluid and v_{sp} is the specific volume. The following correlation was given [47]:

$$\frac{L_{evap}(V_m)^{3/2}}{a_{co}^2} = 3 \tag{1.10}$$

However, later analyses showed that this correlation was not very satisfactory for experimental data. From these analyses it was suggested that there are 13,423,656 layers of molecules in 1 cm^3 of water. In Table 1.3 are given some comparisons of this model of a liquid surface as originally described by Stefan [46].

TABLE 1.3
Enthalpy of Surface Formation, h_s (10^{-14} erg/mol), and Ratios of Evaporation, L_{evap} (10^{-14} erg/mol), at a Reduced Temperature ($T/T_c = 0.7$)

Molecule	h_S	h_S/L_{evap}
Nitrogen	3.84	0.51
Oxygen	4.6	0.50
CCl_4	18.2	0.45
C_6H_6	18.4	0.44
Diethylether	15.6	0.42
ClC_6H_5	20.3	0.42
Methyl formamate	15.4	0.40
Ethyl acetate	18.3	0.4
Acetic acid	11.6	0.34
Water	14.4	0.28
Ethyl alcohol	11.2	0.19
Methyl alcohol	8.5	0.16
Hg	20	0.64

Note: See text for details.

It has been determined that substances that have nearly spherical molecules have Stefan ratios (γ/L_{evap}) of approximately 1/2 (three near neighbors at the surface/six near neighbors in the bulk phase). On the other hand, substances with polar groups on one end give much smaller ratios. This suggests that the molecules are oriented with the nonpolar end toward the gas phase and the polar end toward the bulk liquid phase. At this stage, more detailed analysis is needed to describe these relations in more molecular detail. This also requires a method of measuring the molecular structure, which is lacking at this stage. In spite of this, what one does conclude is that the molecular analysis is valid as regards the surfaces of liquids. Hence, any changes in surface properties would require only molecules at surfaces, as described later below.

It is well-known that both the heat of vaporization of a liquid, ΔH_{vap}, and the ST of the liquid, γ, are dependent on temperature and pressure, and they result from various intermolecular forces existing within the molecules in the bulk liquid. To understand the molecular structure of liquid surfaces, one may consider this system in a somewhat simplified model. The molecular surface energy, S_{mse}, was defined by Eotovos [48] (in 1886) as the surface energy on the face of a cube containing 1 mol of liquid:

$$\Sigma_{mse} = \gamma(M_w v_{sp})^{2/3} \tag{1.11}$$

where
v_{sp} is the specific volume
M_w is the molecular weight

The molar internal heat of evaporation, L_{evap}, can be given as

$$L_{evap} = L_e - \rho M_w(v_G - v_L) \tag{1.12}$$

and

$$\gamma(M_w v_{sp})^{2/3} = 12\ L_{evap} \tag{1.13}$$

The correct value for the molar surface energy is probably not the face of a cube representing the molecular volume:

$$\text{Molecular volume} = M_w(v)^{2/3} \tag{1.14}$$

but rather the area of the sphere containing 1 mol of the liquid

$$\begin{aligned}\text{Molecular surface area} &= 4\pi\left(\frac{3}{4\pi}\right)^{2/3}(M_w v)^{2/3} \\ &= 4.836\ (M_w v)^{2/3}\end{aligned} \tag{1.15}$$

The amount of heat required to convert 1 g of a pure liquid into saturated vapor at any given temperature is called the latent heat of evaporation or latent heat of vaporization, L_{evap}. It has been suggested that

$$\frac{\text{Latent heat of evaporation}}{2\gamma} = \frac{L_{evap}}{2\gamma} \tag{1.15a}$$

$$= \text{Area occupied by all molecules if they lie in the surface} = A_{mol} \tag{1.16}$$

Then we can write

$$\text{Diameter } A_{mol} = v_{sp} \tag{1.17}$$

Hence

$$\text{Diameter} = \frac{2\gamma v_{sp}}{L_{evap}} \tag{1.18}$$

For example, for water

$$\begin{aligned} L_{\text{evap}} &= 600 \text{ g cal}(=0.15 \text{ kg J}) \\ &= 600 \times 42{,}355 \text{ g cm} = 25{,}413{,}000 \text{ g cm} \\ v_{H_2O} &= \text{ca.1 g/cc} \\ \gamma_{oC} &= 88 \text{ dyn/cm} = 88 \text{ mN/m} = 0.088 \text{ N/m} \end{aligned} \tag{1.19}$$

From this we find

$$\begin{aligned} \text{Diameter of water molecule} &= \frac{2 \times 0.088 \times 1}{2{,}541{,}300} = 0.7 \times 10^{-8}\text{cm} \\ &= 0.7 \text{ Å} = 0.07 \text{ nm} \end{aligned} \tag{1.20}$$

which is of the right order of magnitude.

In a later investigation [49], a correlation between heat of vaporization, ΔH_{vap}, and the effective radius of the molecule, R_{eff}, and ST, γ, was found. These analyses showed that a correlation between enthalpy and ST exists which is dependent on the size of the molecule. It thus confirms the molecular model of liquids. More investigations are required at this stage before a molecular model can be delineated.

1.2.4 Effect of Temperature and Pressure on Surface Tension of Liquids

As already mentioned, all natural processes are dependent on the temperature and pressure variations in the environment. For example, the oil reservoirs are found under high temperature (80°C) and pressure (200–300 atm). The molecular interactions in the surface (two dimensional) are by one order of magnitude less than in the bulk (three dimensional). As the temperature increases, the kinetic energy of the molecules increases. This effect thus provides the means of obtaining information about molecular interactions in different systems and interfaces. Molecular phenomena at the surface separating the liquid and the saturated vapor (or the liquid and the walls of its containing vessel) are appreciably more complex than those that occur inside the homogenous liquid, and it is difficult to state much of a rigorous qualitative nature concerning them. The essential difficulty is that from the microscopic standpoint there is always a well-defined surface of separation between the two phases but on the microscopic scale there is only a surface zone, in crossing which the structure of the fluid undergoes progressive modification. It is in this surface zone that the dynamic equilibrium between the molecules of the vapor and those of the liquid is established. Owing to the attractive forces exerted by the molecules of the liquid proper on one another, only the fast-moving molecules can penetrate the layer and escape into the vapor; in the process, they lose kinetic energy and, on the average, attain the same velocity as the molecules in the vapor.

Further, the number of molecules escaping cannot, on the average, exceed the number entering from the much rarer vapor. From a statistical point of view, the density of the fluid is the most important variable in the surface area; it does not, of course, suffer an abrupt change but varies continuously in passing through the surface zone from its value in the liquid to the generally much lower value in the vapor (a decrease by a factor of ca. 1000). In consequence, it is possible to specify only rather arbitrarily where the liquid phase ends and the gaseous phase begins. It is convenient to some extent to define the interface as a certain surface of constant density within the surface zone such that if each of the two phases remains homogeneous up to the surface, the total number of molecules would be the same [7,13].

The work required to increase the area of a surface is the work required to bring additional molecules from the interior to the surface. This work must be done against the attraction of surrounding molecules. Since cohesive forces fall off very steeply with distance between molecules, one can consider as a first approximation interactions between neighboring molecules only. There is strong evidence that the change of density from the liquid phase to vapor is exceedingly abrupt, transitional layers being generally only one or two molecules thick.

Perhaps the most convincing evidence is that derived from the nature of the light reflected from the surfaces of liquids. According to Fresnel's law of reflection, if the transition between air and a medium of refractive index, n, is absolutely abrupt, the light is completely plane polarized if the angle of incidence is the Brucetarian angle. But, if the transition is gradual, the light is elliptically polarized. It was found [22,50] that there is still some small amount of residual ellipticity in the cleanest surfaces of water and that these scatter light to some extent.

The structure of liquid surfaces has been described by using a hybrid approach of thermodynamics and super liquids [20]. Even though the ST phenomenon of liquids has been extensively studied, the transition region, where ST is at present has not been successfully described.

1.2.5 Corresponding States Theory of Liquids

To understand the molecular structure of liquid surfaces, it is important to be able to describe the interfacial forces as a function of temperature and pressure. As temperature increases, the kinetic energy increases due to the increase in the molecular movement. This effect on the change in ST gives information on the surface entropy. Although a large number of reports are found in the literature at this stage, complete understanding of surface energy and entropy has not been achieved. In the following, some of these considerations are delineated. The magnitude of γ decreases almost linearly with temperature within a narrow range [14,36,40]:

$$\gamma_t = \gamma_o(1 - k_o t) \tag{1.21}$$

where
k_o is a constant
t is the temperature (°C)

It was found that the coefficient k_o is approximately equal to the rate of decrease of density (ρ) with rise of temperature:

$$\rho_t = \rho_o(1 - k_d t) \tag{1.22}$$

Values of constant k_d were found to be different for different liquids. Furthermore, the value of k_d was related to T_c (critical temperature) and P_c (critical pressure) [1].

The following equation relates ST of a liquid to the density of liquid, ρ_L, and vapor, ρ_V [51]:

$$\frac{\gamma}{(\rho_L - \rho_V)^4} = C_{mc} = \text{ca. } 3 \tag{1.23}$$

where the value of constant C_{mc} is only nonvariable for organic liquids, while it is not constant for liquid metals.

The effect of temperature (at constant pressure) on ST is different for different fluids (Table 1.4) [5]. This is the surface entropy, s_s ($=-d\gamma/dT$). Thus, we can obtain much useful information from this as regards thermodynamics and the molecular interactions. As shown later, the effect of temperature can also give information about the surface orientation of the molecules.

These data are given here merely to indicate how ST is characteristic for a given fluid, as one can estimate from the effect of temperature. One clearly observes the range in γ and the variation in s_s for the various types of fluids. At the critical temperature, T_c, and the critical pressure, P_c, ρ_c of liquid and vapor is identical; the ST, γ, and total surface energy, like the energy of vaporization, must be zero.

The critical point of the equilibrium of two phases corresponds to the limit of their coexistence. The tension of the interface (ST) decreases as one approaches the critical point and γ becomes zero at this state.

At critical temperature, T_c, and critical pressure, P_c

$$\left(\frac{d\gamma}{dT}\right)_{T \to T_c, P \to P_c} = 0 \tag{1.24}$$

In current literature, erroneously, the term P_c is omitted in this equation [51a]. It also needs to be emphasized that T_c and P_c exist simultaneously, by definition.

TABLE 1.4
Typical Data of Variation of ST with Temperature of Different Liquids

Fluid	T (K)	γ (mN/m)	$(d\gamma/dT)^a$ (dyn/cm/K)
H_2O	293.2	72.8	−0.16
NaCl	1076	114	−0.07
Zn	693.2	782	−0.17
Hg	235.2	498	−0.2

Sources: From Birdi, K.S., ed., *Handbook of Surface & Colloid Chemistry*, CRC Press, Boca Raton, FL, 1997; Birdi, K.S., ed., *Handbook of Surface & Colloid Chemistry-CD Rom*, CRC Press, Boca Raton, FL, 1997; *Handbook of Surface & Colloid Chemistry*, 2nd edn., 2002.

[a] $d\gamma/dT$ is the surface entropy.

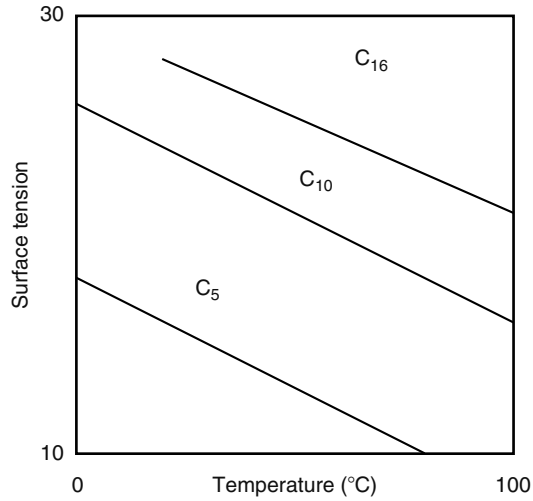

FIGURE 1.10 Variation of ST versus temperature for n_C for *n*-alkanes. (*n*-pentane; *n*-decane; *n*-hexadecane)

At temperatures below the boiling point, which is $2/3\ T$, the total surface energy and the energy of evaporation are nearly constant. The ST, γ, variation with temperature is given in Figure 1.10 for different liquid *n*-alkanes with a number of carbon atoms [52]. These data clearly show that the variation of γ with temperature is a very characteristic physical property of a given liquid, analogous to other bulk properties such as boiling point, heat of vaporization, density, viscosity, compressibility, and refractive index. In other words, the molecules at the surface of the alkanes exhibit dependence on chain length which can be related to some of these bulk properties. The surface entropy is almost a linear function of n_C (Table 1.5). These data provide very useful information about the molecular structures at the surface. This observation becomes even more important when considering that the sensitivity [13,14] of γ measurements can be as high as ca. ± 0.001 dyn/cm (mN/m). It is seen that the magnitude of the extrapolated value of γ at $T = 0°C$ increases with alkane chain length, n_C. This means that γ increases with increasing van der Waals interactions between chains, analogous to heat of vaporization, melting point, and other molecular properties. The data thus show how such useful physical measurements can be related to the molecular property of a homologous series of molecules. This allows one to predict data for more complex molecules. These data clearly show that

TABLE 1.5
Linear Equation a for Data of γ versus Temperature for *n*-Alkanes

Alkane (n_C)	Ao	$B_{s,s}$ ($-d\gamma/dT$)	Extrapolated Value of γ [b]
5	18.25	0.1102	77
6	20	0.1022	75
7	22.10	0.098	76
8	23.52	0.0951	75
9	24.72	0.0935	75
10	25.67	0.092	75
11	26.46	0.0901	75
12	27.12	0.08843	75
13	27.73	0.0872	75
14	28.30	0.0869	75
15	29	0.08565	75
16	29	0.0854	75
17	29	0.0846	75
18	30	0.08423	75
19	30	0.0837	75
20	31	0.0833	75

Note: See text for details.

[a] $\gamma = Ao - B_{S,S}\ T$, where T is in degree Celsius. Magnitude of Ao is the extrapolated value of γ at $T = 0°C$.

[b] At $T = -540°C$ (see text).

the magnitude of γ is proportional to the chain length of the alkanes, n_c. This is to be expected based on the previous relation given by Stefan on the dependence of the magnitude of γ on the heat of evaporation. The data of ST versus temperature can be analyzed as follows. It is well-known that the corresponding states theory can provide much useful information about the thermodynamics and transport properties of fluids. For example, the most useful two-parameter empirical expression that relates the ST, γ, to the critical temperature is given as [4]

$$\gamma = k_o(1 - T/T_c)^{k_1} \tag{1.25}$$

where k_o and k_1 are constants. van der Waals derived this equation and showed that the magnitude of constant $k_1 = 3/2$, although the experiments indicated that $k_1 =$ ca. 1.23. Guggenheim [53] has suggested that $k_1 = 11/9$. Moreover, the quantity $k_o = (V_c)^{2/3/Tc}$ was suggested [54] to have a universal value of ca. 4.4; however, for many liquids, the value of k_1 lies between 6/5 and 5/4. Thus, the correct relation is given as

$$\gamma = \frac{(V_c)^{2/3}}{T_c(1 - T/T_c)^{k_1}} \tag{1.26}$$

It is thus seen that ST is related to T_c and V_c. van der Waals [14,36,40] also found that k_o was proportional to $(T_c)^{1/3}$ $(P_c)^{2/3}$.

The above equation, when fit to the ST, γ, data of liquid CH_4, has been found to give the following relation [55a]:

$$\gamma_{CH_4} = 40.52(1 - T/190.55)^{1.287} \tag{1.27}$$

where $T_{c,CH_4} = 190.55$ K. This equation has been found to fit the γ data for liquid methane from 91°C to −190°C, with an accuracy of ±0.5 mN/m. Although the theory predicts that the exponent is valid only asymptotically close to the critical point, the ST corresponding states theory with additional expansion terms has been shown to be valid for many pure substances over their entire liquid range [55a].

In a different context, the ST of a fluid, γ_a, can be related to that of a reference fluid, γ_{ref}, as follows [55b]:

$$\gamma_a(T) = \left(\frac{T_{a,c}}{T_{ref,c}}\right)\left(\frac{V_{ref,c}}{V_{a,c}}\right)^{2/3}\gamma_{ref}\left(\frac{T_{ref,c}}{T_{a,c}}\right) \tag{1.28}$$

where

T is the temperature

$T_{a,c}$ and $V_{a,c}$ are the critical temperature and volume of fluid under consideration, respectively

Similarly, the terms $T_{ref,c}$ and $V_{ref,c}$ refer to the reference fluid's critical temperature and volume, respectively. This procedure was found to predict the temperature dependence of γ of various fluids and mixtures (such as CO_2, ethane, butane, hexane, octane, hexane + ethane, hexane + CO_2). The variation of γ of a mixture of hexane + ethane was almost linear with the mole fraction of hexane, x_{C6}:

$$\gamma_{C6+C2} = 0.64 + 17.85x_{C6} \tag{1.29}$$

This means that one can estimate the concentration of dissolved ethane from such γ measurements. Similar analyses of $C_6 + CO_2$ data gives almost the same relationship as for $C_6 + C_2H_6$. This indicates that in a mixed system the addition of a gas to a fluid simply reduces the magnitude of γ in the mixture, since the extrapolated plot tends toward almost zero at a mole fraction of the fluid equals zero. That the magnitude of γ of fluids can be measured with a very high accuracy [14] suggests that the solubility of gas (or gases) can be investigated by the γ change. A change in mole fraction by 0.1 unit will give a change in γ of the solution of ca. 2 mN/m. This quantity can be measured with an accuracy of ±0.001 mN/m, suggesting a gas solubility sensitivity of $\pm 10^{-4}$. Further, this method is most useful in those cases where gas is not available in large quantity. This arises from the fact that very small amounts of liquid are needed for γ measurements.

The variation of γ of a large variety of liquids (more than a hundred) is available in literature [52]. The different homolog series will provide information about the stabilizing forces in these fluids. For instance, while alkanes are stabilized by mainly van der Waals forces, the alcohols would be mainly stabilized by both van der Waals forces and hydrogen bonds, the latter being stronger than the former.

To analyze such thermodynamic relations of different molecules, we take the model system to be a homologous series of normal alkanes and alkenes, since very reliable and accurate data are available in the literature. Linear HC chains, *n*-alkanes, are among the most common molecular building blocks of organic matter. They form part of the organic and biological molecules

of lipids, surfactants, and liquid crystals and determine their properties to a large extent. As major constituents of oils, fuels, polymers, and lubricants they also have immense industrial importance. Accordingly, their bulk properties have been extensively studied. The measured variation in γ with temperature data, near room temperature, was almost linear with temperature for all the alkanes with carbon atoms, n_C, from 5 to 18. This means that the magnitude of surface entropy is constant over a range of temperature. Similar observation was made from the analyses of other homolog series of organic fluids (over 100 different molecules):

1. Alkenes [52]
2. *n*-alcohols [52]
3. CO_2 in liquid state [55]

The γ data of alkanes were analyzed by using Equation 1.25. The constants, k_o (between 52 and 58) and k_1 (magnitude ranging between 1.2 and 1.5), were found to be dependent on the number of carbon atoms, n_C; since T_c is also found to be dependent on n_C, the expression for all the different alkanes which individually were fit to Equation 1.29 gave rise to a general equation where γ was a function of n_C and T [14]:

$$\gamma = \text{Function of } T,\ n_C$$
$$= \left(41.41 + 2.731\ n_C - 0.192\ n_C^2 + 0.00503\ n_C^3\right) \tag{1.30}$$

$$1 - \left[\frac{T}{273 + -99.86 + 145.4 \ln (n_C)}\right] + 17.05 \ln\left(n_C^2\right)^{k_1} \tag{1.31}$$

where

$$k_1 = 0.9968 + 0.04087\ n_C - 0.00282\ (n_C)^2 + 0.000844\ (n_C)^3 \tag{1.32}$$

The estimated values from the above equation for γ of different *n*-alkanes were found to agree with the measured data within a few percent: γ for *n*-$C_{18}H_{38}$, at 100°C, was 21.6 mN/m, both measured and calculated (Table 1.6). Using such analyses one does not need to apply tables, since computer memory can assist in the estimation of ST of any alkane at a given temperature. This shows that the ST data of *n*-alkanes fits the corresponding state equation very satisfactorily. In these analyses, the pressure

TABLE 1.6
Calculated[a] γ and Measured Values of Different *n*-Alkanes at Various Temperatures

n-Alkane	Temperature (°C)	γ (Measured)	γ (Calculated)
C_5	0	18.23	18.25
	50	12.91	12.8
C_6	0	20.45	20.40
	60	14.31	14.3
C_7	30	19.16	19.17
	80	14.31	14.26
C_9	0	24.76	24.70
	50	19.97	20.05
	100	15.41	15.4
C_{14}	10	27.47	27.4
	100	19.66	19.60
C_{16}	50	24.90	24.90
C_{18}	30	27.50	27.50
	100	21.58	21.60

Sources: From Birdi, K.S., ed., *Handbook of Surface & Colloid Chemistry*, CRC Press, Boca Raton, FL, 1997; Birdi, K.S., ed., *Handbook of Surface & Colloid Chemistry-CD Rom*, CRC Press, Boca Raton, FL, 1997; *Handbook of Surface & Colloid Chemistry*, 2nd edn., 2002.

[a] From Equation 1.3.

is assumed to be constant. Furthermore, by using this relationship we do not need any elaborate tables of data. Especially by using a simple computer program one can find γ values rapidly and accurately, as a function of both n_C and T. However, the effect of pressure must not be considered as negligible, as delineated later. More studies are needed on similar homolog series of liquids, to understand the relation between molecules and ST.

The physical analyses of the constants k_o and k_1 have not been investigated at this stage. Further, since QSAR models can predict relations between molecular structures and boiling points [56–58], it should be possible to extend these models to ST prediction based upon the above relation. A general and semiempirical correlation between the alkane chain length and ST has been described [59].

It is worth mentioning that the equation for the data of γ versus T for polar (and associating) molecules such as water and alcohols, when analyzed by the above equation, gives magnitudes of k_o and k_1 which are significantly different than those found for nonpolar molecules such as alkanes, etc. This observation therefore requires further analysis to understand the relation among γ, surface entropy, and T_c (as well as P_c and V_c).

The critical constants of a compound are of both fundamental and practical interest. Furthermore, sometimes the critical constants are not easily measured, due to experimental limitation. In Table 1.7, the estimated data for $\gamma_{t=0}$ (at $t = 0°C$) and the magnitude of $d\gamma/dT$ (surface entropy) for a variety of liquids are given. For a very practical approximate estimation of T_c one can use these data as

$$T_c = \frac{\gamma_{t=0}}{(d\gamma/dT)} \tag{1.33}$$

where T is in °C. The calculated value for water is $T_c = 75.87/0.1511 + 273 = 502$ K. This compares with the measured value of 647 K. The data for C_6H_6 gives $T_{c,C_6H_6} = 226.4°C$ (499 K), as compared to the measured value of 561 K. The estimated values are lower as expected.

In the case of *n*-alkanes, the linear part (Figure 1.10) was extrapolated to $\gamma = 0$ to estimate T_c (and $P = 1$ atm). The analyses of the alkane data from C_5 to C_{20} is of much interest in this context, from both a theoretical and practical point of view. If one merely extrapolates the linear part of the measured data (at 1 atm) then the estimated T_c, 1 atm is found to be somewhat lower (ca. 10%, dependent on n_C) than the directly measured values (Table 1.7). It is observed that the magnitudes of T_c for these alkanes can be very high. This may lead, in some cases, to decomposition of the substance if measurements are made directly. On the other hand, if one can use the present ST data to estimate T_c then it can provide much useful information.

The difference between the estimated T_c (lower in all cases) and the measured T_c (range measured from 200°C to 500°C at P_c) per carbon atom is found to be 6°. This gives values of estimated T_c within a 5% error for alkanes with n_C from 5 to 20. This finding is of great significance.

TABLE 1.7
Comparison of Measured and Estimated[a] Values of $T_{c,\ 1atm}$ at $\gamma = 0$ for Different *n*-Alkanes[b]

n_C	$T_{c,\ \gamma\ =\ 0}$ (°C) (Estimated)	$T_{cc,at\ Pc}$ (Measured)	D[c]	D/n_C[d]	P_c/Bar (Measured)
5	166	197	31	6	33
6	200	234	34	6	30
7	216	267	51	7	27
8	240	296	56	7	25
9	260	320	60	7	23
10	279	344	65	6.5	21
11	294	364	70	6.3	20
12	307	385	78	6	19
13	318	403	85	6	17
14	326	420	94	6	14
15	336	434	98	6	15
16	342	449	107	6	14
17	350	460	110	6	13
18	356	475	119	6	12
19	361	483	121	6	11
20	367	494	127	6	11

[a] From γ versus T data to $\gamma = 0$.
[b] Extrapolated from data for γ versus T.
[c] $T_c, \gamma \to_o - T_{c,estimated}$.
[d] $T_c, \gamma \to_o - T_{c,estimated}/n_C$.

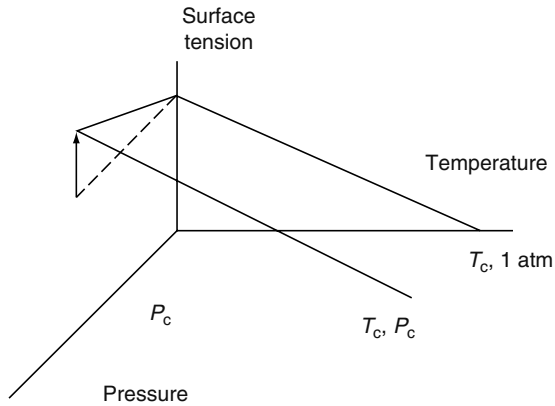

FIGURE 1.11 Variation (schematic) of ST versus temperature (T) and pressure (P).

One of the most important consequences is that, in the case of fluids that are unstable at high temperatures, one need only measure the variation of ST with temperature, from which one can estimate the value of T_c. The correction required arises from the effect of P_c on γ.

One can thus show from these data that for *n*-alkanes:

$$T_{c,\gamma 0} = T_c - n_C 6 \tag{1.34a}$$

Or, one can rewrite

$$T_c = T_{c,\gamma 0} + n_C 6 \tag{1.34b}$$

This shows convincingly that an increase in pressure gives rise to an increase in ST, that is, $d\gamma/dP = +$ (i.e., positive). However, the need for this correction is expected; if we consider the fact that at the critical point the pressure is not 1 atm but P_c, then a correction would be needed. For example, the T_c and P_c for alkanes of n_C equal to 12 and 16 are 658 K and 18 atm and 722 K and 14 atm, respectively. In fact, all the relations as found in literature which neglect critical pressure are inadequate.

To modify the data of γ versus T at 1 atm to include the effect of pressure, P_c, then this would give an increase in ST, since the quantity $d\gamma/dP$ is positive for liquids [16]. In other words, the analyses of ST versus temperature data must be reformulated to include the effect of P_c on the ST data, as shown below (Figure 1.11). The measured γ data is obtained at 1 atm.

The extrapolated line is moved from 1 atm to P_c and moved up by a value which corresponds to $d\gamma/dP$ (positive). It is thus possible to estimate the magnitude of $d\gamma/dP$ from such data.

The correction required based on the above is as follows:

$$T_c = \frac{(\gamma_{t,ref} + s_s t_{ref})}{s_s} + 6(n_C) \tag{1.35}$$

where

$\gamma_{t,ref}$ is the ST at a given temperature (and at 1 atm)
s_s is the surface entropy

The correction term, second on the right-hand side, arises from the correction necessary to obtain γ at T_c at pressure equal to P_c. Previous studies have shown that an increase in the hydrostatic pressure over gas–water systems can produce marked changes in the ST by virtue of enhanced adsorption of the gaseous component at the interface.

It is obvious that when more systematic ST data becomes available, a more detailed molecular description of the significance of this observation can be given. For example, there exist no such analyses of alkane mixtures (of two or more components). These latter systems are of much interest in enhanced oil-recovery processes (EOR).

The γ versus temperature data for the homologous series *n*-alkanes and *n*-alkenes show some unique characteristics. The data for alkanes, on extrapolation to a hypothetical supercooled region, converge at T_{sc} = ca. −540°C, and $\gamma_{sc} = 75$ mN/m [1a,b]. The calculated values of γ_{sc} are given in Table 1.8 for a homologous series of alkanes. The magnitude of γ_{sc} is estimated as ca. 75 mN/m in all cases. This shows that the alkane molecules in their hypothetical supercooled state at T_{sc} (−540°C = 2(−273°C) exhibit the same ST ($\gamma_{sc} = 75$ mN/m) regardless of chain length. To analyze this in more detail, the ST data of alkenes were investigated [16]. These data also exhibit a supercooled temperature, T_{sc} (≅ −540°C), where all the alkene

TABLE 1.8
Effect of Alkyl Chain Length (n_C) on the Variation of γ versus T for Homologous Series of Alkanes or Alkenes and Other Fluids

Homologous series variation of γ with temperature and n_C	
Alkanes convergence (at $\gamma = 75$ mN/m and -540°C)	
Alkenes convergence (at $\gamma = 75$ mN/m and -540°C)	
Complicated alkyl-derivatives	Divergence at lower temperature
	Convergence at ca. 120°C and $\gamma =$ ca. 30 mN/m

molecules have the same γ_{sc} (75 mN/m). This characteristic property can be ascribed to the fact that long molecule axes will tend to lie along a preferred direction at the interface. This is well recognized in such structures as liquid crystal phases. Thus, at the supercooled state at T_{sc} (-540°C), the attractive forces and the repulsive forces in different alkanes exhibit a supercooled state where the dependence on n_C disappears. In other words, all alkanes behave as pseudomethane. Another possibility could be that the holes in the alkanes are all filled at a supercooled state, T_{sc}, as expected from Eyring's [60a] theory for liquids.

From these observations, one can rewrite Equation 1.35 in the case of *n*-alkanes data relating T_c to s_s and the above supercooled point:

$$\begin{aligned} T_c &= \gamma_{sc}/s_s + 6n_C + T_{sc} \\ &= 75/s_s + 6n_C - 540 \end{aligned} \tag{1.36}$$

where $T_{sc} = -540$°C. From this relation, one can estimate the values of T_c (within a few percentage accuracy) if one knows s_s (or if variation of γ is known for any temperature). Since the change in γ with temperature can be measured with a very high sensitivity (± 0.001 mN/m), then one can estimate T_c with a very high accuracy. Considering, that it is not easy to determine T_c of liquids as easily (and accurately) as γ. Of course, currently these analyses have been found to be valid only for *n*-alkanes with chain lengths from $n_C = 5$ to 20. This observation has many useful aspects. It shows that the concepts as described here as regards the molecular structures of liquids is fairly accurate. Further, the correlation between surface entropy and critical temperature has much theoretical value, especially in all kinds of theoretical model considerations.

The variation of surface entropy for molecules with complex stabilizing forces other than alkanes requires extensive analysis at this stage, although preliminary analysis shows that for more complicated molecules such as alkyl-naphthalene or alkyl-diester homologous series the plots of γ versus temperature intersect at ca. 30 dyn/cm and 150°C [16].

The γ versus temperature data for complicated homolog series molecules also showed that molecular packing changes as the alkyl chain changes in a different manner than in the case of simple alkane molecules. This is as expected, since the molecules are interacting under different kinds of forces. The effect of a change in the alkyl chain length will also be different than in the case of linear alkanes. The data plots do not converge at lower temperatures, as was observed for alkanes and alkenes. The data, however, do indeed show that the molecules at the surface exhibit the same magnitude of ST (i.e., ca. 30 mN/m at 120°C) regardless of the alkyl chain length. Observation of a variety of homologous series of molecules allows us to conclude that the hydrophobic effect arising from the addition of each CH_2 group gives rise to three general types of γ versus temperature data plots (Table 1.8). The following observations are of importance when considering the effect of hydrophobicity on γ and s_s:

1. *n*-Alkanes and *n*-alkenes: ST increases from 18.25 to 29.18, while surface entropy decreases from 0.11 to 0.0854 for C_5 to C_{16}.
2. Alkyl-phosphonates: ST decreases from 39.15 to 30.73 mN/m, while surface entropy decreases from 0.126 to 0.0869 for C_1–C_8-phosphonates.
3. Dialkyl-phosphonates and alkyl-diesters: Same trend as for alkyl-phosphonates. These observations require further theoretical analysis at this stage; however, it is sufficient to stress that the method to extrapolate the data to hypothetical states is justified in the case of alkanes and alkenes.

ST of any fluid can be related to various interaction forces, for example, van der Waals, hydrogen bonding, dipole, and induction forces. The above analyses of the alkanes thus provide information about the van der Waals forces only. In other homologous series, such as alcohols, we can expect that there are both van der Waals and hydrogen bonding contributions. One can thus combine these two kinds of homologous series of molecules and analyze the contribution from each kind of interaction. The magnitude of ST, γ, has also been calculated from statistical theory and molecular orientations at the free surface in nematic liquid crystals [60b]. These calculations were carried out based on a model of the mean field approximation

in the system of rod-like molecules interacting via attraction as well as hard-core repulsion. Excluded volume effect was found to give favorable results as regards the alignment of molecules at the free surface. Experimental data [61] have shown that one observes a jump in the ST, T_c; however, the estimation of the jump in ST was considerably larger than the experimental data.

Since the shape of molecules is known to affect the thermodynamic properties of real fluids and fluid mixtures, more investigations are necessary. This arises from the fact that all intramolecular forces are dependent on the distance between the molecules. Hence, in the case of nonspherical or asymmetric-shaped molecules the distance will be dependent on the nonsymmetrical surfaces of the molecule. ST measurements are thus found to provide much useful information about this aspect.

In the studies of ST of liquids, one needs data for calibration of instruments at different temperatures. The variation of γ for water with temperature, t(°C), is given as follows by various investigators.

By Harkins [5],

$$\gamma_{\text{water}} = 75.680 - 0.138t - 0.05356t^2 + 0.0647t^3 \tag{1.37}$$

The high accuracy is important in such data, since we use these for calibration purposes. More recent and reliable data by Cini et al. [62] indicates that

$$\gamma_{\text{water}} = 75.668 - 0.1396t - 0.2885\ 10^{-3}t^2 \tag{1.38}$$

where t is in °C.

The surface entropy, S_s, corresponding to the above equation is

$$\begin{aligned} S_s &= \frac{-d\gamma}{dT} \\ &= k_1 k_o (1 - T/T_c) k_1 - 1/(T_c) \end{aligned} \tag{1.39a}$$

and the corresponding expression for surface enthalpy, H_s, is

$$H_s = \gamma - T\left(\frac{d\gamma}{dT}\right) \tag{1.39b}$$

$$= k_o(1 - T/T_c)k_1 - 1[1 + (k_1 - 1)T/T]_c \tag{1.40}$$

ST is a type of Helmholtz free energy, and the expression for surface entropy is $s_s = -d\gamma/dT$. Hence, an amount of heat (H_s) must be generated and absorbed by the liquid when the surface is extended. The reason why heat is absorbed upon extending a surface is that the molecules must be transferred from the interior against the inward attractive force to form the new surface. In this process, the motion of the molecules is retarded by this inward attraction, so that the temperature of the surface layers is lower than that of the interior, unless heat is supplied from outside [4,7].

These analyses thus confirm the assumptions made regarding the molecular structure of the interfacial region as compared to the bulk phase. The surface entropy provides a very useful description of the molecular interactions in the interface of a liquid. The values of surface entropy ($-d\gamma/dT$ at 0°C) for a range of liquids are given in Table 1.9. The data clearly show how the surface entropy describes the molecular properties of the different liquids (as expected). The magnitude of surface entropy varies from 0.07 to 0.16 mN/mT.

The following ST data for benzene (C_6H_6) and ethyl ether are analyzed by using the above relations for estimating T_c. The ST data measured under pressure close to T_c are compared with the estimated values (Table 1.10). This analysis clearly shows that more investigations are necessary in this area of research.

In a recent study [36], a new model of fluids was described by using the generalized van der Waals theory. Actually, van der Waals over 100 years ago suggested that the structure and thermodynamic properties of simple fluids could be interpreted in terms of separate contributions from intermolecular repulsions and attractions. A simple cubic equation of state was described for the estimation of the ST. The fluid was characterized by the Lennard-Jones (12-6) potential. In a recent study the dependence of ST of liquids on the curvature of the liquid–vapor interface has been described [53b].

1.2.6 Surface Tension of Liquid Mixtures

All industrial liquid systems are made up of more than one component, which makes the studies of mixed liquid systems important. Further, the natural oil consists of a variety of alkanes (besides other organic molecules). The analyses of ST of

TABLE 1.9
Magnitudes of ST, γ (mN/m) and Surface Entropy[a] for Different Liquids

Liquid	ST	$-d\gamma/dT$
H_2O	75.87	0.1511
CS_2	35.71	0.1607
CH_3OH	23.5	0.071
C_2H_5OH	23.3	0.080
C_3H_7OH	25.32	0.081
C_4H_9OH	26.11	0.081
$C_2H_4(OH)_2$	49.34	0.0935
Glycerol	65.28	0.0598
$[C_2H_5]_2O$	19.31	0.117
C_6H_6	31.7	0.140
Toluene	30.76	0.115
o-Xylene	31.06	0.107
m-Xylene	29.7	0.106
p-Xylene	29.31	0.115
Hexane	21.31	0.1032
Octane	23.36	0.092
Decane	23.76	0.084
$CHCl_3$	28.77	0.1134
C_2H_5I	33.53	0.137
$[CH_2Cl]_2$	35.31	0.139
$[CH_2Br]_2$	40.51	0.131
CH_3NO_2	36.69	0.146
$C_2H_5NO_2$	34.92	0.120
Methyl formate	28.50	0.157
Ethyl formate	26.30	0.136
Ethyl acetate	26.84	0.127
Amyl acetate	27.04	0.098
Ethyl propionate	5.73	0.111
Ethyl malonate	33.6	0.100
C_6H_5CN	40.9	0.117
Furfurol	43.5	0.096
Thiophene	33.5	0.113
Pyridine	38.1	0.136
Picoline	36.6	0.118
Quinoline	47.0	0.122
Piperidine	30.6	0.118
Benzamide	47.20	0.070
Phenylhydrazine	44.02	0.076

[a] $-d\gamma/dT$ at 0°C.

liquid mixtures (e.g., two or three or more components) has been the subject of studies in many reports [8,13,53a,b,54,63–69]. According to Guggenheim's [53a,b] model of liquid surfaces, the free energy of the molecule is

$$G_i = k_B T \ln(a_i) \tag{1.41}$$

where a_i is the absolute activity. This latter term can be expressed as

$$a_i = N_i g_i \tag{1.42}$$

where

N_i is the mole fraction (unity for pure liquids)
g_i is the derived from the partition function

TABLE 1.10
ST Data of C_6H_6 and Ethylether at Different Temperatures[a]

	ST			
	C_6H_6		$(C_2H_5)_2$ O	
Temperature (°C)	Measured (Under Pressure)	Estimated (at 1 atm)	Measured	Estimated
0	31.7	31.7	19.31	19.31
20	28.88	30.06	17.01	16.97
50	—	—	13.60	13.46
61	23.61	23.16	—	—
110	—	—	7.00	6.44
120	16.42	14.9	—	—
140	—	—	4.00	2.93
170	—	—	1.42	−0.58
180	9.56	6.5	—	—
240	3.47	−1.9	—	—
$T_c = 288.5$	0	−8.7	—	—
$T_c = 193$	—	—	0	−3.3

[a] Measured and estimated from data in Table 1.9.

The free energy can thus be rewritten as

$$\begin{aligned} G_i &= g_i s_i \\ &= k_B T \ \ln\left(\frac{a_1}{a_1^s}\right) \end{aligned} \tag{1.43}$$

where s_1 is the surface area per molecule. This is the free energy for bringing the molecule, a_1, from the bulk to the surface, a_1^s. In a mixture consisting of two components, 1 and 2, we can then write the free energy terms as follows for each species:

$$\gamma s_1 = k_B T \ln\left(N_1 g_1 / N_1^s / g_1^s\right) \tag{1.44}$$

and

$$\gamma s_2 = k_B T \ \ln\left(N_2 g_2 / N_2^s / g_2^s\right) \tag{1.45}$$

where N^s is the mole fraction in the surface such that

$$N_1^s + N_2^s = 1 \tag{1.46}$$

As a first approximation one may assume that $s = s_1 = s_2$; that is, the surface area per molecule of each species is approximately the same. This will be reasonable to assume in such cases as mixtures of hexane + heptane, for example. This gives

$$\gamma_s = k_B T \ \left[\ln\left(N_1 g_1 g_1^s\right) + \ln\left(N_2 g_2 / g_2^s\right)\right] \tag{1.47}$$

or, in combination with Equation 1.42, one can rewrite as follows:

$$\exp\left(\frac{-\gamma_s}{k_B T}\right) = N_1 \exp\left(\frac{-\gamma_1 s}{k_B T}\right) + N_2^2 \exp\left(\frac{-g_2 s}{k_B T}\right) \tag{1.48}$$

Hildebrand and Scott [54] have given a more expanded description of this derivation.

Using the regular solution theory [53a,b], the relation between activities was given as

$$RT \ \ln f_1 = -a_1 \ N_2^2; \quad RT \ \ln f_2 = -a_1 \ N_1^2 \tag{1.49}$$

where f_1 denotes the activity coefficient. Other analyses by later investigators [65] gave a different relationship:

$$\gamma_{12} = \gamma_1 N_1 + \gamma_2 N_2 - \beta N_1 N_2 \tag{1.50}$$

where β is a semiempirical constant.

The STs of a variety of liquid mixtures, such as carbon tetrachloride–chloroform, benzene–diphenylmethane, and heptane–hexadecane [64], have been reported.

In the case of some mixtures, a simple linear relationship has been observed:

1. Water-*m*-dihydroxy-benzene (resorcinol) in the range of 0.1–10.0 M concentration gives following relationship [70a]:

$$\gamma = 72.75 - 8.0\ (M_{\text{resorcinol}})\ (\text{at } 20^\circ\text{C}) \tag{1.51}$$

2. *Iso*-octane-benzene mixtures: The ST changes gradually throughout. This means that the system behaves almost as an ideal.
3. Water–electrolyte mixtures: The example of water–NaCl shows that the magnitude of ST increases linearly from ca. 72 to 80 mN/m for 0 to 5M NaCl solution (dγ/dmol NaCl = 1.6 mN/mol NaCl) [70b]:

$$\gamma_{\text{NaCl}} = 72.75 + 1.6\ (M_{\text{NaCl}})\ (\text{at } 20^\circ\text{C}) \tag{1.52}$$

   In another system, for water–NH_4NO_3:

$$\gamma_{NH_4NO_3} = 72.75 + 1.00\ (M_{NH_4NO_3})\ (\text{at } 20^\circ\text{C},\ m < 2\ m) \tag{1.53}$$

   It is seen that increase in γ per mole added NaCl is much larger (1.6 mN/m mol) than that for NH_4NO_3 (1.0 mN/m mol). In general, the magnitude of ST of water increases on the addition of electrolytes, with a very few exceptions. This indicates that the magnitude of surface excess term is different for different solutes. In other words, the state of solute molecules at the interface is dependent on the solute. In a recent study a ST model for concentrated electrolyte solutions by the Pitzer equation was described [70b].
4. *n*-butanol/water (Table 1.11) and *n*-hexanoic acid/water mixture data have been also analyzed [16a,71,72]. Some theoretical analyses of ST data has been given in recent reports [68a,b]. However, there is a need for investigations that should help in the usefulness of this relation and data [68b].

The data of other diverse mixtures include the following:

1. Ethanol–water mixtures and hydrogen bonding: The ethanol–water mixture is known to be the most extensively investigated system. The addition of even small amounts of ethanol to water gives rise to contraction in volume [73]. A remarkable decrease of the partial molar volume of ethanol with a minimum at an ethanol molar fraction of 0.08 was observed. The same behavior is observed from heat-of-mixing data. The ST drops rather appreciably when 10%–20% ethanol is present, while the magnitude of ST slowly approaches that of the pure ethanol.
2. ST of HC + alcohol mixtures: The ST of the binary HC (benzene, toluene, cyclohexane, methyl cyclohexane) + alcohol (ethanol, *t*-pentyl alcohol) mixtures were reported [74] at 303.15 K (30°C).

The effect of temperature on the ST of mixtures of *n*-propanol/*n*-heptane has been investigated [75,76a]. The variation of ST by temperature (K) for pure components was

TABLE 1.11
ST of *n*-Butanol Solutions at 25°C

ST	Butanol (mol)							
	0.00329	0.00658	0.01320	0.0264	0.0536	0.1050	0.2110	0.4330
γ	72.80	72.26	70.82	68.00	63.14	56.31	48.08	38.87

Sources: From Birdi, K.S., ed., *Handbook of Surface & Colloid Chemistry*, CRC Press, Boca Raton, FL, 1997; Birdi, K.S., ed., *Handbook of Surface & Colloid Chemistry-CD Rom*, CRC Press, Boca Raton, FL, 1997; *Handbook of Surface & Colloid Chemistry*, 2nd edn., 2002.

$$\gamma_{\text{propanol}} = 25.117 - 0.0805(T - 273.15) \tag{1.54}$$

$$\gamma_{\text{heptane}} = 22.204 - 0.1004(T - 273.15) \tag{1.55}$$

It is seen that the effect of temperature is lower on a more stable structure as propanol (due to hydrogen bonding) than in heptane, as expected. In a recent study, the refractive indices and STs of binary mixtures of 1,4-dioxane + *n*-alkanes at 298.15 K were analyzed [76b].

The ST of binary mixtures of water + monoethanolamine and water + 2-amino-2-methyl-1-propanol and tertiary mixtures of these amines with water from 25°C to 50°C have been reported [76c]. The ST of aqueous solutions of diethanolamine and triethanolamine from 25°C to 50°C has been analyzed [76d].

1.2.7 Solubility of Organic Liquids in Water and Water in Organic Liquids

The process of solubility of one compound into another is of fundamental importance in everyday life: examples include industrial applications (paper, oil, paint, washing) and pollution control (oil spills, waste control, toxicity, biological processes such as medicine). Accordingly, many reports are found in the literature that describes this process both on a theoretical basis and by using simple empirical considerations. As already mentioned, the formation of a surface or interface requires energy; however, how theoretical analyses can be applied to curvatures of a molecular-sized cavity is not satisfactorily developed. It is easy to accept that any solubility process is in fact the procedure where a solute molecule is placed into the solvent where a cavity has to be made. The cavity has both a definite surface area and volume. The energetics of this process is thus a surface phenomenon, even if of molecular dimensions (i.e., nm^2). Solubility of one compound, S, in a liquid such as water, W, means that molecules of S leave their neighbor molecules (SSS) and surround themselves by WWW molecules. Thus, the solubility process means formation of a cavity in the water bulk phase where a molecule, S, is placed (WWWSWWW). Langmuir [16] (and some recent investigators) suggested that this cavity formation is a surface free energy process for the solubility.

The solubility of various liquids in water and vice versa is of much interest in different industrial and biological phenomena of everyday importance. In any of these applications, one would encounter instances where a prediction of solubility would be of interest; the following such applications are mentioned of general interest. Furthermore, solubilities of molecules in a fluid are determined by the free energy of solvation. In more complicated processes such as catalysis, the reaction rate is related to the desolvation effects. A correlation between the solubility of a solute gas and the ST of the solvent liquid was described [77,78] based on the curvature dependence of the ST for C_6H_6, C_6H_{12}, and CCl_4. This was based on the model that a solute must be placed in a hole (or cavity) in the solvent.

The change in the free energy of the system, ΔG_{sol}, transferring a molecule from the solvent phase to a gas phase is then

$$\Delta G_{\text{sol}} = 4\pi r^2 \gamma_{\text{aq}} - e_{\text{i}} \tag{1.56}$$

where e_{i} is the molecular interaction energy. By applying the Boltzmann distribution law:

$$\frac{c_{\text{gs}}}{c_{\text{g}}} = \exp\left(\frac{\Delta G_{\text{G}}}{k_{\text{B}} T}\right) \tag{1.57}$$

where

c_{gs} is the concentration of gas molecules in the solvent phase
c_{g} is their concentration in the gas phase

Combining these equations, we obtain

$$\ln\left(\frac{c_{\text{g}}^{\text{s}}}{c_{\text{g}}}\right) = \left(\frac{-4\pi r^2 \gamma_{\text{aq}}}{k_{\text{B}} T}\right) + \frac{e_{\text{i}}}{k_{\text{B}} \text{T}} \tag{1.58}$$

This model was tested for the solubility data of argon in various solvents, where a plot of log (Ostwald coefficient) versus ST was analyzed. In the literature, similar linear correlations were reported for other gas (e.g., He, Ne, Kr, Xe, O_2) solubility data (schematic plot in Figure 1.12).

The solubility of water in organic solvents does not follow any of these aforementioned models. For instance, while the free energy of solubility, ΔG_{sol}, for alkanes in water is linearly dependent on the alkyl chain, there exists no such dependence of water solubility in alkanes (and therefore clearly needs to be investigated) [16].

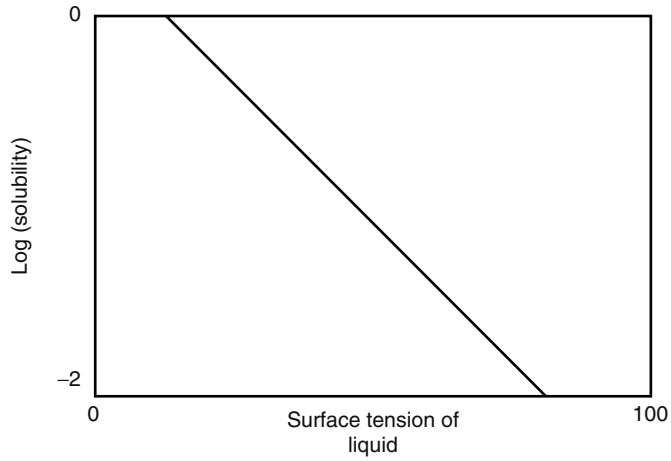

FIGURE 1.12 Solubility of gas versus ST of liquids.

If the microscopic IFT determines the work of forming a cavity in alkane then this should be almost the same as the cavity needed in alkane for dissolution of water. Furthermore, very few data in literature are available as regards the effect of temperature or pressure on the solubility.

1.2.8 Hydrophobic Effect

In general, all natural processes are dependent on the physicochemical properties of water (especially when considering that over 70% of the earth is covered by water). Amphiphile molecules, such as long-chain alcohols or acids, lipids, or proteins, exhibit polar–apolar characteristics, and the dual behavior is given this designation. The solubility characteristics in water are determined by the alkyl or apolar part of these amphiphiles which arise from hydrophobic effect [16,79–81]. Hydrophobicity plays an important role in a wide variety of phenomena, such as solubility in water of organic molecules, oil–water partition equilibrium, detergents, washing and all other cleaning processes, biological activity, drug delivery, and chromatography techniques. Almost all drugs are designed with a particular hydrophobicity as determined by the partitioning of the drug in the aqueous phase and the cell lipid-membrane.

The ability to predict the effects of even simple structural modifications on the aqueous solubility of an organic molecule could be of great value in the development of new molecules in various fields, for example, medical or industrial. There exist theoretical procedures to predict solubilities of nonpolar molecules in nonpolar solvents and for salts or other highly polar solutes in polar solvents, such as water or similar substances [82a]. However, the prediction of solubility of a nonpolar solute in water has been found to require some different molecular considerations.

Furthermore, the central problems of living matter comprise the following factors:

- Recognition of molecules leading to attraction or repulsion
- Fluctuations in the force of association and in the conformation leading to active or inactive states
- Influence of electromagnetic or gravitational fields and solvents including ions, and electron or proton scavengers

In the case of life processes on earth, one is mainly interested in solubility in aqueous media.

The unusual thermodynamic properties of nonpolar solutes in aqueous phase were analyzed [82b], by assuming that water molecules exhibit a special ordering around the solute. This water-ordered structure was called the iceberg structure. The solubility of semipolar and nonpolar solutes in water has been related to the term molecular surface area of the solute and some IFT term [83]. This model was later analyzed by various investigators in much greater detail [16,84–87].

On the basis of Langmuir–Herman–Amidon model, the solubility, X_{solute}, in water was given by the following expression for the free energy:

$$RT\ (\ln X_{\text{solute}}) = -(\text{Surface area of solute})\ (\gamma_{\text{sol}}) \tag{1.59}$$

where ST, γ_{sol}, is some micro-IFT term at the solute–water (solvent) interface.

The quantity surface area of a molecule is the cavity dimension of the solute when placed in the water media. The conformational potential energy of a molecule is, in general, consists of various parameters [88]:

- Nonbonded energy
- Electrostatic energy
- Strain energy associated with the stretching of bonds
- Strain energy due to bending of bonds
- Torsional potential
- Hydrogen bond formation energy

Further, in the simple HCs, since there is not very much stretching or bending deformation, the van der Waals interactions are the most important. The rotations about near-single bonds, the nonbonded interactions, make the major contributions to the torsional potential. The surface areas of the solutes have been calculated by computer programs [86–89].

The data of solubility, total surface area (TSA), and HC surface area (HYSA) are given in Table 1.12 for some typical alkanes and alcohols [16]. The relationship between different surface areas of contact between the solute solubility (sol) and water were derived as [87]:

$$\ln(\text{sol}) = -0.043\ \text{TSA} + 11.78/(RT)$$
$$\Delta G_{\text{o,sol}} = -RT\ln(\text{sol}) = 25.5\ \text{TSA} + 11.78 \tag{1.60}$$

where sol is the molar solubility and TSA is in Å^2.

The quantity 0.043 ($RT = 25.5$) is some micro-ST. The micro-ST has not been analyzed exhaustively at the molecular level. Especially, the effect of temperature and pressure needs to be investigated. It is also important to mention that at molecular level there cannot exist any surface property which can be uniform in magnitude in all directions. Hence, the micro-ST will be some average value. The effect of temperature also must be investigated [16].

TABLE 1.12
Solubility Data, Boiling Point, Surface Areas[a], and Predicted Solubility[b] of Different Molecules in Water[c]

Compound	Solubility (Measured[Molal])	TSA	OHSA	Boiling Point	Solubility Predicted (Molal)
n-butane	2.34E–3	255.2	—	—	1.43E–3
Isobutane	2.83E–3	249.1	—	—	1.86E–3
n-pentane	5.37E–4	287	—	—	3.65E–4
2-Methylbutane	6.61E–4	274	—	—	6.21E–4
3-Methylpentane	1.48E–4	300	—	—	2.08E–4
Neopentane	7.48E–4	270	—	—	7.52E–4
Cyclohexane	6.61E–4	279	—	—	5.11E–4
Cycloheptane	3.05E–4	301.9	—	—	1.92E–4
Cyclooctane	7.05E–5	322.6	—	—	7.89E–5
n-Hexane	1.11E–4	310	—	—	1.23E–4
n-Heptane	2.93E–5	351	—	—	2.33E–5
n-Octane	5.79E–6	383	—	—	5.87E–6
n-Butanol	1.006	272	59	118	0.82
2-Butanol	1.07	264	43	100	1.5
n-Pentanol	0.255	304	59	138	0.21
n-Hexanol	0.06	336	59	157	0.053
Cyclohexanol	0.38	291	50	161	0.43
n-heptanol	0.016	368	59	176	0.014
1-Octanol	0.0045	399	59	195	0.00345
1-Nonanol	0.001	431	59	213	0.00088
1-Decanol	0.0002	463	59	230	0.000224
1-Dodecanol	2.3E–5	527	59	—	1.43E–5
1-Tetradecanol	1.5E–6	591	59	264	9.4E–7
1-Pentadecanol	5E–7	623	59	—	2.4E–7

Note: $\text{Å} = 10^{-8}\ \text{cm} = 10^{-10}\ \text{m}$.

[a] TSA and OHSA in Å^2 units.

[b] Calculated from Equation 1.65.

[c] At 25°C.

In the case of alcohols, assuming a constant contribution from the hydroxyl group, the HYSA = TSA–OSHA:

$$\ln(\text{sol}) = -0.0396\ \text{HYSA} + 8.94 \tag{1.61}$$

However, one can also derive a relationship which includes both HYSA and OHSA (hydroxyl group surface area):

$$\ln(\text{sol}) = 0.043\ \text{HYSA} - 0.06\ \text{OHSA} + 12.41 \tag{1.62}$$

The relations described above did not give correlations to the measured data which were satisfactory (ca. 0.4–0.978). The following relationship was derived based on the solubility data of both alkanes and alcohols, which gave correlations on the order of 0.99:

$$\ln(\text{sol}) = 0.043\ \text{HYSA} + 8.003\ \text{IOH} - 0.0586\ \text{OHSA} + 4.42 \tag{1.63}$$

where the IOH term equals 1 (or the number of hydroxyl groups) if the compound is an alcohol and zero in the absence of the hydroxyl group.

The term HYSA thus can be assumed to represent the quantity that relates to the effect of the HC part on the solubility. The effect is negative, and the magnitude of t is 17.7 erg/cm^2.

The magnitude of OHSA is found to be 59.2 Å^2. As an example, the surface areas of each carbon atom and the hydroxyl group in the molecule 1-nonanol were estimated (Table 1.13) [16]. It is seen that the surface area of the terminal methyl group (84.9 Å^2) is approximately three times larger than the methylene groups (31.82 Å^2, or 31.82 10^{-20} m^2).

The solubility model was tested for the prediction of a complex molecule such as cholesterol [87]. The experimental solubility of cholesterol is reported to be ca. 10^{-7} M. The predicted value was ca. 10^{-6} (TSA = 699 Å^2). It is obvious that further refinements are necessary for predicting the solubilities of such complex organic molecules.

The molecular surface areas are still not easily available, even though computer computations have been carried out to some extent [87–89]. However, all these analyses were reported at some temperature in the vicinity of room temperature. The effect of temperature and other parameters such as pressure has not been extensively reported.

Computer simulation techniques have been applied to such solution systems [88b,c]. The Monte Carlo statistical mechanics have provided much useful information about the energetics, structure, and molecular interactions. The computations suggested that at the hexanol–water interface minimal water penetration into the HC regions takes place.

The surface area model for solubility in water or any solvent can be further investigated by measuring the effect of temperature or added salt. Preliminary measurements indicate that some of the above models are not completely satisfactory. One finds that the solubility of butanol in water decreases while the magnitude of ST of aqueous NaCl solution increases. These kinds of data are of much importance for such systems as EOR. At present, recovery of oil in general is between 30% and 70%.

TABLE 1.13
Surface Areas (A^2) of Each Methylene and Methyl Group in 1-Nonanol

CH_3–CH_2–CH_2–CH_2–CH_2–CH_2–CH_2–CH_2–CH_2–OH

Group	Surface Area at the Interface between Solute and Solvent
OH	59.15
C_1	45.43
C_2	39.8
C_3	31.82
C_4	31.82
C_5	31.82
C_6	31.82
C_7	31.82
C_8	42.75
C_9	84.92

Note: See text for details.

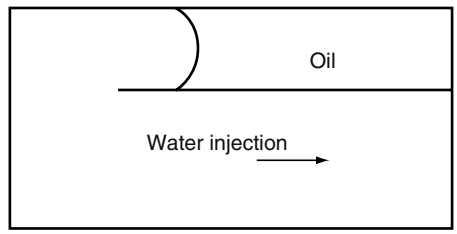

FIGURE 1.13 Oil–water system in a reservoir.

As is well known [16], the bilayer structure of cell membranes exhibits hydrophobic properties in the HC part. This means that those molecules which must interact with the membrane's interior must be hydrophobic. Anesthesia is brought about by the interaction between some suitable molecule and the lipid molecules in the biological membrane at the cell interface. The effect of pressure has been reported to be due to the volume change of membranes, which reverses the anesthesia effect. Local anesthetics are basically amphiphile molecules of tertiary amines, and some of them have colloidal properties in aqueous solution. Anesthetic power is determined by the hydrophobic part of the molecule. ST measurements showed a correlation with the anesthetic power for a variety of molecules: dibucane < tetracainebupivacainemepivacaine < lidocaine < procaine (all as HCl salts) [90].

1.3 INTERFACIAL TENSION OF LIQUIDS (LIQUID$_1$–LIQUID$_2$)

1.3.1 INTRODUCTION

The interfacial forces present between two phases, such as immiscible liquids, are of much importance from a theoretical standpoint, as well as in regard to practical systems. The liquid$_1$–liquid$_2$ interface is an important one as regards such phenomena as chemical problems, extraction kinetics, phase transfer, emulsions (oil–water), fog, and surfactant solutions. In the case of primary oil production, one has to take into consideration the ST of oil. On the other hand, during a secondary or tertiary recovery, the IFT between the water phase and oil phase becomes an important parameter. For example, the bypass and other phenomena such as snap-off are related to the interfacial phenomena [91]. This phenomenon is illustrated in Figure 1.13.

The magnitude of ΔP across the water phase is lower than in the oil–reservoir phase, which results in that oil gets trapped while water injection produces only water (or very little oil production).

Analogous examples can be given for other systems, such biliquid flow-through porous media, where again IFT considerations would be required (ground–water pollution control). It is thus obvious that other multicomponent flow systems will be much complicated phenomena. This is also relevant in the case of blood flow through arteries. Notwithstanding, data on interfaces and IFT is not found in many textbooks that cover important aspects of liquids [40]. Furthermore, although the concept of hydrophobicity in single-component systems such as alkanes has been extensively described, these properties for two-phase systems, such as oil–water, have almost not been described in detail in current literature [16]. The problem of liquid$_1$–liquid$_2$ interfaces is of interest to both theoreticians and experientialists. Indeed, over the past decades a great effort has been expended in trying to understand and give plausible theories from a statistical–mechanical point of view [53a]. The interface can be considered as being where the molecules of different phases meet and the asymmetrical forces are present (Figure 1.14).

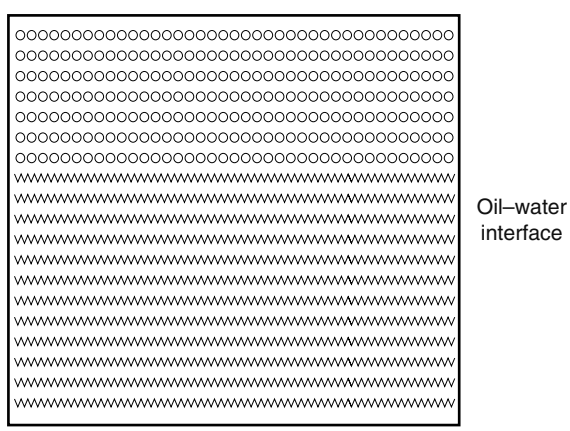

FIGURE 1.14 Interfacial region (schematic) at two liquids (O, oil phase; W, water phase).

The molecules in the bulk phases are surrounded by alike molecules. However, at the interface the molecules are subjected to interactions with molecules of phase O and from phase W. Since the molecules in both phases are situated at the interface, the orientations may not exactly be the same as when inside the bulk phase. IFT between two liquids is less than the ST of the liquid with the higher ST, because the molecules of each liquid attract each other across the interface, thus diminishing the inward pull exerted by that liquid on its own molecules at the surface. The precise relation between the STs of the two liquids separately against theory vapor and the IFT between the two liquids depends on the chemical constitution and orientation of the molecules at the surfaces. In many cases, a rule proposed by Antonow holds true with considerable success [53a].

The various kinds of interfacial forces have been described in the literature [16]. The interface at the water and simple aromatic HCs hydrogen bonding has been considered [92–96]. The IFT of water–alkanes and water–aromatic HCs has been extensively analyzed. These analyses have been considered for two different kinds of forces: short-range and long-range work of adhesion.

1.3.2 Liquid–Liquid Systems—Work of Adhesion

The free energy of interaction between dissimilar phases is the work of adhesion, W_A (energy per unit area):

$$W_A = W_{AD} + W_{AH} \tag{1.64}$$

where W_A is expressed as the sum of different intermolecular forces as follows: [16,94]:

London dispersion forces, D
Hydrogen bonds, H
Dipole–dipole interactions, DD
Dipole-induced interactions, DI
Π-bonds, Π
Donor–acceptor bonds, DA
Electrostatic interactions, EL

It is also easily seen that the W_{AD} term will always be present in all systems (i.e., liquids and solids), while the other contributions will be present to a varying degree as determined by the magnitude and nature of the dipole associated with the molecules.

To simplify the terms given by the above equation, one procedure has been to compile all the intermolecular forces arising from the dipolar nature of W_{AP}:

$$W_A = W_{AD} + W_{AP} \tag{1.65}$$

where

$$W_{AP} = W_{AH} + W_{ADD} + W_{AID} \tag{1.66}$$

The molecular description of dispersion forces has been given in much detail in the literature. The calculated value of ST of *n*-octane was analyzed from these parameters.

The calculated value for γ of octane = 19.0 mN/m, while the measured value is 21.5 mN/m, at 20°C (i.e., $\gamma_{octane} = \gamma_{LD}$). The real outcome of this example is that such theoretical analyses do indeed predict the surface dispersion forces, γ_{LD}, as measured experimentally, to a good accuracy. In a further analysis, the Hamaker constant, A_i, for liquid alkanes is found to be related to γ_{LD} as

$$A_i = 3 \times 10^{-14}(\gamma_{LD})^{11/12} \tag{1.67}$$

This was further expanded to include components at an interface between phases I and II:

$$A_{I,II} = 3 \times 10^{-14}/e_2\left(\sqrt{\gamma_I^D} - \sqrt{\gamma_{II}^D}\right)^{11/6} \tag{1.68}$$

where e_2 is the dielectric constant of phase 2; however, in some cases, forces other than dispersion forces would also be present [94].

The manifestation of intermolecular forces is a direct measure of any interface property and requires a general picture of the different forces responsible for bond formation, as discussed in the following:

1. Ionic bonds: The force of attraction between two ions is given as

$$F_{\text{ion}} = \frac{(g^+ g^-)}{r^2} \tag{1.69}$$

and the energy, U_{ion}, between two ions is related to r_{ion} by the equation as

$$U_{\text{ion}} = \frac{(g^+ g^-)}{r_{\text{ion}}} \tag{1.70}$$

where two charges (g^+, g^-) are situated at a distance of r_{ion}.
2. Hydrogen bonds: On the basis of molecular structure, those conditions under which hydrogen bonds might be formed are (1) presence of a highly electronegative atom, such as O, Cl, F, and N, or a strongly electronegative group such as $-CCl_3$ or –CN, with a hydrogen atom attached; (2) in the case of water, the electrons in two unshared sp^3 orbitals are able to form hydrogen bonds; (3) two molecules such as $CHCl_3$ and acetone (CH_3COCH_3) may form hydrogen bonds when mixed with each other, which is of much importance in interfacial phenomena.
3. Weak-electron sharing bonding: In magnitude, this is of the same value as the hydrogen bond. It is also the Lewis acid–Lewis base bond (comparable to Brønsted acids and bases). Such forces might contribute appreciably to cohesiveness at interfaces; a typical example is the weak association of iodine (I_2) with benzene or any polyaromatic compound. The interaction is the donation of the electrons of I_2 to the electron-deficient aromatic molecules (π-electrons).
4. Dipole-induced dipole forces: In a symmetrical molecule, such as CCl_4 or N_2, there is no dipole ($ma = 0$) through the overlapping of electron clouds from another molecule with dipole, mb, with which it can interact with induction. The typical magnitudes of the different forces are given in Table 1.14 for comparison. It will thus be clear that various kinds of interactions would have to be taken into consideration whenever we discuss IFTs of liquid–liquid or liquid–solid systems [16,94–96].

1.3.3 Interfacial Tension Theories of Liquid–Liquid Systems

As shown above, various types of molecules exhibit different intermolecular forces, and their different force and potential-energy functions can be estimated [16]. If the potential-energy function were known for all the atoms or molecules in a system, as well as the spatial distribution of all atoms, it could in principle then be possible to add up all the forces acting across an interface.

Further, this would allow one to estimate the adhesion or wetting character of interfaces. Because of certain limitations in the force field and potential-energy functions, this is not quite so easily attained in practice. Further, the microscopic structure at a molecular level is not currently known. For example, to calculate the magnitude of ST of a liquid, one needs knowledge of the radial pair-distribution function. However, for the complex molecule, this would be highly difficult to measure, although data for simple liquids such as argon have been found to give the desired result. The intermolecular force in saturated alkanes arises

TABLE 1.14
Intermolecular and Interatomic Forces between Molecules

Energy	Force (kJ/mol)
Chemical bonds	
Ionic	590–1050
Covalent	60–700
Metallic	100–350
Intermolecular forces	
Hydrogen bonds	50
Dipole–dipole	20
Dispersion	42
Dipole-induced dipole	2.1

TABLE 1.15
Values of the ST (γ) Components (γ_L, γ_{LD}, γ_{LP}) of Some Test Liquids 20°C

Liquids	γ_L	γ_{LD}	γ_{LP}
al-Br-naphthalene	44.4	44.4	≈0
Diiodomethane	50.8	50.8	≈0
Dimethyl sulfoxide	44	36	8
Ethylene glycol	48	29	19
Glycerol	64	34	30
Formamide	58	39	19
Water	72	21.8	51

only from London dispersion forces. Now, at the interface, the HC molecules are subjected to forces from the bulk molecule, equal to γ (see Figure 1.14). Also, the HC molecules are under the influence of London forces due to molecules in the oil phase. It has been suggested that the most plausible model is the geometric means of the force due to the dispersion attraction, which should predict the magnitude of the interaction between any dissimilar phases.

As described earlier, the molecular interactions arise from different kinds of forces, which mean that the measured ST, γ, arises from a sum of dispersion, γ_D, and other polar forces, γ_P:

$$\gamma = \gamma_D + \gamma_P \tag{1.71}$$

Here, γ_D denotes the ST force solely determined by the dispersion interactions, and γ_P arises from the different kinds of polar interactions (Equation 1.66). Some values of typical liquids are given in Table 1.15.

The IFT between HC and water (W) can be written as

$$\gamma_{HC,W} = \gamma_{HC} + \gamma_W - 2(\gamma_{HC}\gamma_{W,D})^{1/2} \tag{1.72}$$

where subscripts HC and W denote the hydrocarbon and water phases, respectively. Considering the solubility parameter analysis of mixed-liquid systems, we find that the geometric mean of the attraction forces gives the most useful prediction values of IFT. Analogous to that analysis in the bulk phase, the geometric mean should also be preferred for the estimation of intermolecular forces at interfaces. The geometric mean term must be multiplied by a factor of 2 since the interface experiences this amount of force by each phase. However, the relation in Equation 1.72 was alternatively proposed by Antonow [16]:

$$\begin{aligned}\gamma_{12} &= \gamma_1 + \gamma_2 - 2(\gamma_1\gamma_2)^{1/2} \\ &= \left[(\gamma_1)^{1/2} - (\gamma_2)^{1/2}\right]^2\end{aligned} \tag{1.73}$$

This relation is found to be only an approximate value for such systems as fluorocarbon- or HC–water interfaces, while not applicable to polar organic liquid–water interfaces. The effect of additives such as *n*-alkanols on the IFT of alkane–water interfaces has been investigated in much detail [97].

To analyze these latter systems, a modified theory was proposed. The expression for IFT was given as [98,99]

$$\gamma_{12} = \gamma_1 + \gamma_2 - 2\Phi(\gamma_1\gamma_2)^{1/2} \tag{1.74}$$

where the value of Φ varied between 0.5 and 0.15. Φ is a correction term for the disparity between molar volumes of v_1 and v_2. This theory was extensively analyzed in literature and satisfactory agreement was found with experimental data [16].

1.3.4 Hydrophobic Effect on the Surface Tension and Interfacial Tension

In most systems, it is of interest to determine how a change in the alkyl part of the organic molecule (i.e., the hydrophobic part) affects the surface and IFT. In spite of its importance (both in biology and technical industry), no such systematic analysis is found in the current literature. These molecular considerations are pertinent in any reaction where the hydrophobicity might be of major importance in the system; Examples include surfactant activity, EOR, protein structure and activity, and pharmaceutical molecules and activity.

TABLE 1.16
Variation of γ (IFT) with Alkyl Chain Length and Temperature

n_C/T(°C)	20	30	35
6	50.8	49.92	49.49
8	51.68	50.78	50.31
12	52.78	51.99	51.50
14	53.32	52.46	52.04
16	53.77	52.9	—

The hydrophobic interactions are known to control many aspects of self-assembly and stability of macromolecular and supramolecular structures [16]. This has obviously been useful in both theoretical analysis and technical development of chemical structures. Furthermore, the interaction between nonpolar parts of amphiphiles and water is an important factor in many physicochemical processes, such as surfactant micelle formation and adsorption or protein stability. To make the discussion short, this interaction is discussed in terms of the measured data of the surface and IFT of homologous series. Analysis has shown that there is no clear correlation; therefore, different homologous series are discussed separately.

Data concerning the IFT of an alkane–water system deserves detailed analysis for various basic theoretical reasons. Not only are these systems of fundamental importance in oil recovery processes and emulsion formation but such molecules also form the basis of structures in complex biological and industrial molecules.

These systems also provide an understanding of the molecular basis of interfaces, since the amphiphile molecules consist of alkyl chains and hydrophilic groups. Thermodynamic analyses on surface adsorption and micelle formation of an anionic surfactants in water were described by ST (drop volume) measurements [16]. These IFT data are analyzed in Table 1.16. These data show that at 20°C (Table 1.17) the magnitude of ST changes nonlinearly (varying from 1.7 to 0.7 mN/m per CH_2) with alkyl chain length. IFT changes linearly with a magnitude of 0.3 mN/m (dyn/cm) per CH_2 group. These data can be compared (Table 1.18) with a homolog series of aromatic compounds.

ST changes with a magnitude of ca. 0.3 mN/m per CH_2 group. This is much lower than for *n*-alkanes. The change in IFT per CH_2 group is rather large in comparison with the alkane versus water data. The latter values are approximately five times larger. This shows that the simple dependence of the hydrophobic effect on the number of carbon atoms becomes rather complicated when considering the interfacial properties. These differences thus may be suggestive of the differences in orientation of the alkyl chains at the interfaces. This subject has been recently investigated by measuring ST and IFT near the freezing point of the oil (alkanes) phase under supercooled measurements, as described further below.

In Table 1.19, data of IFT of the alcohol versus water system are analyzed. The variation of IFT with a change in alkyl chain length for different organic liquids versus water is given in Table 1.20. These data clearly show that simple hydrophobic correlations with alkyl chain length as observed in bulk phases [16,79a] are not found at interfaces and require further analysis. IFT analysis of organic mixtures has been reported [62b].

The protein molecules exhibit hydrophobicity due to polar and apolar side chains [16]. The protein denaturation process has been analyzed by considering the enthalpy of fusion of the hydrophobic groups when undergoing transfer from the liquid organic phase to water phase [100,101]. The hydrophobic effect is recognized to play an important role in such biological systems.

TABLE 1.17
ST (γ) and IFT of n-Alkane/Water Systems

Organic Liquid	ST	IFT	$d\gamma/CH_2$	$d\gamma_{IFT}/CH_2$
n-C_6	18.0	50.7	—	—
n-C_7	19.7	51.2	1.7	0.5
n-C_8	21.4	51.5	1.7	0.3
n-C_{10}	23.5	52.0	1.1	0.3
n-C_{12}	25.1	52.2	0.8	0.1
n-C_{14}	25.6	52.8	0.3	0.3
n-C_{16}	27.3	53.3	0.85	0.3

TABLE 1.18
ST (γ) and IFT of Aromatic Compounds versus Water Organic ST IFT

Liquid	ST	IFT	γ_{ST}/CH_2	$d\gamma_{IFT}/CH_2$
C_6H_6	28.88	33.90	—	—
$CH_3C_6H_5$	28.5	36.1	−0.38	2.2
$C_2H_5C_6H_5$	29.2	38.4	+0.7	2.3
$C_3H_7C_6H_5$	28.99	39.60	−0.2	1.2

Note: See text for details.

1.3.5 Heat of Fusion in the Hydrophobic Effect

In some studies [101] it has been pointed out that, when one calculates the hydrophobic effect in protein denaturation, the enthalpy of fusion of the hydrophobic groups should be considered. Similar analysis had been given in earlier hydrophobic interactions analysis [100]. In a later study, a model for absolute free energy of solvation of organic, small inorganic, and biological molecules in aqueous media was described [102]. From the Monte Carlo simulation studies of aqueous solvation and the hydrophobic effect, one assumes that some 250 or more solvent molecules are involved in the process [103–105]. To resolve this problem, the so-called self-consistent field solvation model for the hydrophobic effect was described [102].

1.3.6 Analysis of the Magnitude of the Dispersion Forces in Water (γ_D)

As water plays a very important role in a variety of systems encountered in everyday life, its physicochemical properties are of much interest. Therefore, the magnitude of water γ_D has been the subject of much investigation and analysis. By using Equation 1.72 and the measured data of IFT for alkanes–water, the magnitude of γ_D has generally been accepted to be 21.8 mN/m (at 25°C). The most convincing data on this value is supported from the measured and the calculated value of contact angle at octane–Teflon–water [16]. This value, however, has been questioned by other investigators. The criticism arises from the observation that data of IFT and Equation 1.72 do not give a linear plot for $(\gamma_2 - \gamma_{12})/\gamma_1$ versus $(\gamma_1 - 1)$, and the plots did not seem to intercept the theoretical origin at 0, −1. Additionally, it has been shown that the value of γ_{LD} as calculated from Equation 1.74 for water is not independent of the alkane chain length; however, other investigators [106] have shown that the following relationship is valid. A plot of $W_A = 2(\gamma_{1,LD}{}^{1/2}\gamma_{2,LD})^{1/2}$ versus $\gamma^{1/2}$ is linear:

$$W_A = 6.6\gamma_1 + 12.0 \tag{1.75}$$

where γ_1 is in mN/m units. These observations are consistent with a value of $\gamma_{2,D} = 10.9$ mN/m and the presence of a residual interaction over the interface, possibly resulting from the Debye forces of 12.0 mN/m. However, this appears unlikely since theoretical calculations [16] convincingly give a value of 19.2 mN/m for $\gamma_{2,D}$ ($\gamma_{water,D}$), and Debye forces could only contribute about 2 mN/m.

Assuming that alkane molecules lie flat at the interface, the additive contributions from the $-CH_3$ and $-CH_2-$ group to W_A are given by [106]

$$W_A = \frac{[2W_{CH_3} - \sigma_{CH_3} + (N-2)\sigma_{CH_2}W_{CH_2}]}{(N-2)\sigma_{CH_3} + 2\sigma_{CH_2}} \tag{1.76}$$

TABLE 1.19
ST (γ) and IFT of Alcohol versus Water System (25°C)

Organic Liquid	ST	IFT	$d\gamma_{ST}/CH_2$	$d\gamma_{IFT}/CH_2$
n-butyl alcohol	24.6	1.8	—	—
n-amyl alcohol	25.7	4.4	1.1	2.6
n-hexyl alcohol	24.5	6.8	−1.2	2.4
n-heptyl alcohol	25.8	7.7	1.3	0.9
n-octyl alcohol	27.5	8.5	1.7	0.8

TABLE 1.20
Change in IFT per -CH_2- group for Various Organic Liquids versus Water (25°C)

Organic Liquid	Change in IFT/CH_2 Group	
	Short Chain	Long Chain
Alkanes	0.5	0.3
Alcohols	2.5	1
Phenyl	2.2	—

Note: See text for details.

where

N denotes the number of carbon atoms in the alkane chain

s denotes the surface area for $-CH_3$ (0.11 nm^2) or $-CH_2$ (0.05 nm^2) groups

The values for work of adhesion for $-CH_3$ and $-CH_2-$ groups are estimated to be 30 mN/m $= W_{CH_3}$ and 52 mN/m $= W_{CH_2}$, respectively. The plots of γ_{12} versus N using Equation 1.74 show that the relation given in Equation 1.76 for a flat alkane orientation model at the interface is in agreement with the experimental data. This suggests that the magnitude of γ_D for water is 19.5 mN/m, which is in agreement with the experimental data.

To obtain any thermodynamic information of such systems, it is useful to consider the effect of temperature on IFT. The alkane–water IFT data has been analyzed.

These data show that IFT is lower for C_6 (50.7 mN/m) than for the other higher chain length alkanes. The slopes (interfacial entropy, $-d\gamma/dT$) are all almost the same, ca. 0.09 mN/m per CH_2 group. This means that water dominates the temperature effect, or that the surface entropy of IFT is determined predominantly by the water molecules. Further, as described earlier, the variation of ST of alkanes varies with chain length. This characteristic is not present in IFT data; however, it is worth noticing that the slopes in IFT data are lower than that of both pure alkanes and water. The molecular description needs to be analyzed at this stage in the literature.

It may be safe to conclude that the magnitude of different IFTs (e.g., dispersion tension of water) might be constant; however, there is much need for a more thorough analysis.

As mentioned earlier, simple specular reflection profiles can yield detailed interfacial structural information [107]. X-ray and neutron reflectometers have been developed specifically to investigate the liquid surfaces [107,108]. The problem is to be able to study the buried interfacial region by x-ray methods. The beam of x-rays or thermal neutrons are thus required to impinge on the sample at low angles ($<10°$). This also requires that the top phase is made as thin as possible to avoid significant absorption or incoherent scattering. The two systems studied were [107,109a]

1. Cyclohexane–water
2. Cyclohexane–water (with surfactant)

These studies showed that the interfacial region is very diffuse and that the major excess electron density arises from the nonaqueous phase of the interface. The thickness of the layer in the presence of a surfactant was found to be of the magnitude 15.4 Å (1.54 nm).

1.3.7 Surface Tension and Interfacial Tension of Oil–Water Systems

The oil–water interface is one of the most important systems (as found in all emulsions). The liquid–liquid interface constitutes a phase separation where two different molecules meet. One can directly measure the magnitude of the ST, with a rather very high precision. It would thus seem that much useful information can thus be obtained if one could measure some dynamic parameter of interface, such as the freezing phenomena. It is widely known that liquids can be cooled below their freezing temperature without solidification (supercooled fluid) and that they can be heated above heir boiling temperature without vaporization (superheated liquid).

The behavior of liquid surfaces near the freezing point or under supercooled conditions has not been investigated in much detail. Although the subject is fundamental and of considerable intrinsic importance in science and technology, it remains severely underinvestigated because the traditional techniques have been difficult to apply definitively. As is well-known, most liquids will undergo supercooling when the temperature is lowered slowly below the freezing point. It is also known that crystallization takes place at surfaces under cooling. So much so that liquids such as water will not freeze until $-40°C$ under

strict controlled conditions and purity. Other fluids exhibit similar supercooled behavior: benzene to −8°C and glycerol to −40°C [16]. Under these conditions, the liquid remains homogeneous beyond the line of phase equilibrium into the so-called metastable region.

This is important, as it is well recognized that supercooled liquids may be regarded as legitimate representatives of the liquid state [110]. The limit of supercooling has also been of some interest, as surely liquids must solidify before absolute temperature. In fact, the liquid state in comparison to the gas state is stabilized due to gravity forces. Thus, the supercooled state is a quite legitimate phase of interest for the fundamental understanding of phase equilibria. Furthermore, the crystallization requires the necessary orientation before the phase change.

It has been argued [111] that supercooled liquids should be considered as legitimate representatives of the liquid state. The fact that a phase exists with a lower Gibbs energy than the liquid, so that a spontaneous transformation (i.e., crystallization) is possible, although in some cases it may even be slow, is not an inherent property of the liquid state and according to some views may be discarded. The analysis given above on the ST of alkanes, alkenes, and other liquids thus provides support to these postulates.

As mentioned above, the ST of all liquids decreases with a rise in temperature. On the other hand, it was also observed that the ST of a supercooled liquid passes continuously through the freezing point [112].

Recent studies have shown that the ST of fluids near their freezing point can provide useful molecular information [113a,b]. From both x-ray scattering and γ measurements, it was concluded that abrupt formation of a crystalline monolayer on the surface of *n*-alkanes, *n*-$C_{20}H_{44}$, took place above their bulk melting temperatures [113a]. The abrupt change in γ at 38.6°C was suggested to indicate the solid monolayer formation. The bulk solidification was observed at 35.6°C, after which the Wilhelmy plate provides no useful information. In Figure 1.15, a schematic description is given. From these studies, it was concluded that a layering transition on the free surface of fluid alkanes at temperatures a few degrees above their solidification is observed. The surface exhibited a single monolayer of alkane forms in an apparently first-order transition with hexagonal packing structure and chains oriented vertically.

It was also found that the freezing of lower chain alkanes, such as *n*-hexadecane, $C_{16}H_{34}$, did not show an abnormal ST behavior. The ST data for hexadecane [113b,16a] has been described elsewhere. The crystallization of a mixture of 90% C_{16} + 10% C_{14} was also investigated. These data showed that crystallization takes place at 15.5°C, which is lower than that for pure C_{16}. The IFT of the water–alcohol (with 10–15 carbon atoms) interface was investigated near the crystallization temperature [114] The water–undecanol data [115] indicated that a phase transition occurred a few degrees above the melting point (11°C) of the alcohol.

Furthermore, the process of melting, is to be regarded as the transition of a substance from a state of order to one of disorder among the molecules. In a recent investigation [16,113b], the effects of additives to the aqueous phase on the IFT, γ, versus temperature curves near the freezing point of *n*-hexadecane were reported. The aim of these investigations was to determine the effect of additives such as proteins which are surface active on the supercooled region and the IFT. This would reveal the effect of the adsorbed protein molecule on the IFT of the water–alkane system and could be used as a model for cell membranes [17].

The IFT versus temperature curves for different systems have been investigated: C_{16} versus water, C_{16} versus an aqueous solution with protein (BSA; casein). These data showed that the freezing of *n*-hexadecane takes place at 18°C; however, the supercooling is observed down to 16.6°C. In contrast, ST measurements at the air–liquid interface showed no supercooling behavior [16a].

The slope of the data, $d\gamma/dT$, is of the same value (ca. −0.09 mN/m) as reported in literature for a C_{16}–water system. In other words, the magnitude of the IFT of the system increases as temperature decreases. After reaching the supercool

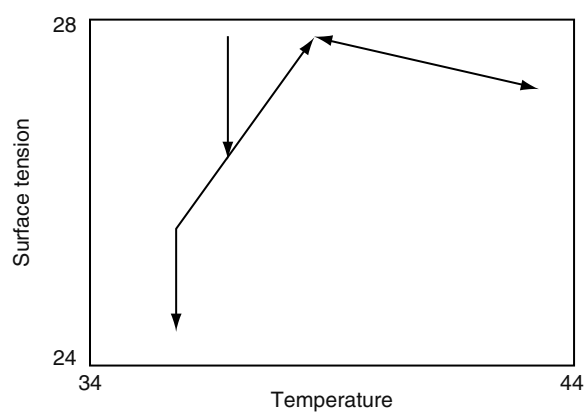

FIGURE 1.15 Variation of γ of long-chain alkane in heating and cooling cycles (schematic). The arrows indicate the temperature scan direction.

temperature (16.6°C), as the crystallization starts the temperature increases. C_{16} is still in a liquid state, as the value of the IFT also abruptly decreases until it reaches the freezing point, 18°C. These data show, for the first time, that fluids crystallize in the bulk phase in a different way than in the surface. The large change in IFT after freezing is due to the solidification and inability of the Wilhelmy plate method to provide any useful information for such solid–oil systems. The abrupt change observed under the supercooled process must be investigated by high-speed measurements. This could provide information about the dynamics of surface molecules. The data also show that the scatter in the plots is reduced after freezing initiates at ca. 16.5°C. Very fast data acquisition has been attempted on these systems. The rate of crystallization is very fast and could not be determined successfully.

Crystallization is known to initiate at the interface. It is thus obvious that the crystallization will then be dependent on the magnitude of IFT. The water–hexadecane interface will not be able to freeze exactly at the freezing point of hexadecane (18°C) because of the neighboring water molecules. However, at the supercooled temperature of 16°C, it seems that water molecules have no effect or a lesser effect on the packing of the hexadecane chains at the interface, which means that the bulk structure of hexadecane and the interfacial phase is similar, and the freezing can take place. The supercooling is also observed with protein (BSA, casein, lactoglobulin) in addition to the aqueous phase-C_{16} system, but the freezing point of hexadecane increases to 18.2°C. This indicates that the crystallization of the hexadecane is affected by the presence of surface-active molecules. The supercooling will have extensive dependence on various interfaces, such as emulsions, oil recovery, and immunological systems. The adsorption of proteins from aqueous solutions on surfaces has been studied by Neutron reflection [116a]. It is known that polymer/surfactant complexes are formed at the water/air interface, as studied by ST and x-ray reflectivity studies [116b]. Furthermore, the effect of ST on the stability of proteins has been described in terms of a molecular thermodynamics model [116c]. Further studies are needed before a more plausible description can be given as to how the protein molecules affect the freezing point. Many studies fast data acquisition (ca. 1/10 s/ data point) has indeed indicated that the transition from liquid to solid at interfaces is very complex [16].

These studies provide a view of the structure and molecular interactions in interfacial regions of more complicated systems, such as monolayer, bilayer, and biphase systems. The two-dimensional assemblies are thus subject to the water molecule effect in the packing energetics. In the future, the rate of the supercooled region should be investigated in more detail. This has much interest for the physicochemical understanding of the kinetics of phase change processes. The velocity being related to the cluster formation might be useful in the estimation of impurities.

1.4 LIQUID–SOLID SYSTEMS (CONTACT ANGLE–WETTING–ADHESION)

The state of liquid in contact with a solid surface is of much importance in many everyday phenomena (detergency, adhesion, friction, wetting, flotation, suspensions, solid emulsions, erosion, printing, pharmaceutical products). If one considers two systems, such as a drop of liquid (water) placed on different solid surfaces (glass, Teflon), one observes the following. The contact angle, θ (Figure 1.16), as defined by the balance between surface forces (STs) between the respective phases, solid (γ_S), liquid (γ_{liquid}) and LS (liquid–solid) (γ_{SL}) [12,16,109c,117–125]:

$$\gamma_S = \gamma_{SL} + \gamma_{liquid} \cos\theta \tag{1.77}$$

In the case of water–glass and water–Teflon, one finds that the magnitude of θ is 30° and 105°, respectively. Since the liquid is the same, the difference in contact angle arises from the different solid STs. From this, one can therefore easily see that the ST of solid is an important surface parameter. A more extensive analysis can be found elsewhere [16,117–125].

Recent studies by using scanning probe microscopy [127], which is based on using a sharp tip to measure and investigate solid surfaces (with nanometer resolution). In a recent study, the contact angles of individual colloidal spheres (4.4 μm) were

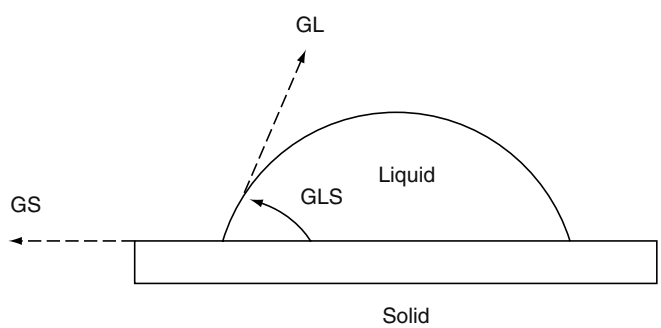

FIGURE 1.16 Contact angle at the liquid–solid interface. (GS/GL/GLS = solid/liquid/solid–liquid/ ST).

measured. These data were compared with contact angles obtained on similarly prepared planar surfaces. The particles were attached to atomic force microscope cantilevers. The force between the particle in aqueous medium and an air bubble was measured versus the distance. From the resulting force curves, the magnitude of contact angles and detachment forces of single particles were estimated. Contact angles of gold-coated silica particles were adjusted between 20° and 100° by SAMs from different mixtures of undecanethiols and hydroxy undecane thiols from solution. In parallel, contact angles on flat gold surfaces prepared in the same way were determined by the sessile drop method. A systematic difference between contact angles measured with particles and on planar surfaces was observed. Results are discussed in terms of line tension of the three-phase contact line. In addition, detachment forces were measured. Detachment forces were slightly higher than predicted from flotation theory. This might be caused by a pinning of the three phase contact line. Further, the relation between Young's equilibrium contact angle and the hysteresis on rough paraffin wax surfaces was investigated [128]. Advancing and receding contact angles (contact angle hysteresis) of four organic liquids and water were measured on a variety of polymer surfaces and silicon wafers using an inclinable plane [129]. The magnitude of contact angles varied widely from liquid to liquid and from surface to surface. Surface roughness was relatively unimportant. Instead, the contact angles seemed to be more closely tied to the chemical nature of the surfaces. In general, contact angles increased with the liquid ST and decreased with the ST of the solid. Several definitions were used to calculate contact angle hysteresis from the experimental data. Although hysteresis is usually considered an extensive property, we found that on a given surface a wide range of liquids gave a unique value of reduced hysteresis. Apparently, reduced hysteresis represents an intrinsic parameter describing liquid–solid interactions.

A generalized drop length–height method has been described for the determination of contact angle in the drop-on-fiber systems [130]. The procedure was found to overcome many of the difficulties found in the application of the maximum drop length–height method to determine the contact angle. It was also found that the method can be applied to a large part of a drop profile for the calculation, which reduces the statistical error of the determination and thus provides higher reliability and accuracy. This study reported investigations based on both the theoretically simulated and the experimentally obtained drop profiles. The accuracy was reported to be in order of 0.5%–1% for the drop profiles of usual experimental quality, which can be obtained using common digital image processing hardware and software.

In recent years, a series of studies have been reported on the dynamic systems where a drop of liquid is placed on a smooth solid surface [117–125]. The system of liquid drop–solid is a very important system in everyday life. For example, this is significant in rain drops placed on tree leaves or other surfaces. It is also significant in all kinds of systems where a spray of fluid is involved, such as in sprays or combustion engines, etc. Further, in many diagnostics devices (such as blood analyses etc.), enzymes are applied in very small amounts (microliter) from solutions as a drop on an electrode. This means that after evaporation of the fluid the remaining enzyme must be well described for the diagnostic instrument to function reliably, The dynamics of a liquid drop evaporation rate is of much interest in many phenomena (combustion engines; rain drops and environment; aerosols and pollution). The liquid–solid interface can be considered as follows. Real solid surfaces are, of course, made up of molecules not essentially different in their nature from the molecules of the fluid. The interaction between a molecule of the fluid and a molecule of the boundary wall can be regarded as follows. The position of the molecule in the solid state is not as mobile as those of the fluid. It is therefore permissible for most purposes to regard the molecules in solid state as stationary. However, complexity arises in those liquid–solid systems where a layer of fluid might be adsorbed on the solid surface, such as in the case of water–glass.

Systematic studies have been reported in the literature on the various modes of liquid drop evaporation when placed on smooth solid surfaces [117–125]. In these studies, the rate of the mass and contact diameter of water and *n*-octane drops placed on glass and Teflon surfaces were investigated. It was found that the evaporation occurred with constant spherical cap geometry of the liquid drop. The experimental data supporting this were obtained by direct measurement of the variation of the mass of droplets with time and as well as by the observation of contact angles. A model based on the diffusion of vapor across the boundary of a spherical drop was considered to explain the data. Further studies were reported, where the contact angle of the system was $\theta < 90$. In these systems, the evaporation rates were found to be linear and the contact radius constant. In the latter case, with $\theta > 90°$, the evaporation rate was nonlinear, the contact radius decreased and the contact angle remained constant.

As a model system, one may consider the evaporation rates of fluid drops placed on polymer surfaces in still air [109d]. The mass and evaporating liquid (methyl acetoacetate) drops on polytetrafluoroethylene (Teflon) surface in still air have been reported. These studies suggested two pure modes of evaporation: at constant contact angle with diminishing contact area and at constant contact area with diminishing contact angle. In this mixed mode, the shape of the drop would vary resulting in an increase in the contact angle with a decrease in the contact circle diameter, or, sometimes a decrease in both quantities. These investigators developed a theory to predict the evaporation rate and residual mass at any time in the life of the drop based on the spherical cap geometry. In a later study [125], the change in the profile of small water droplets on poly(methyl methacrylate) due to evaporation in open air. The drops were observed to maintain a constant contact radius over much of the evaporation time. Measurements were carried out of θ and the drop height, h_d, as a function of time in the regime of constant contact radius.

The results showed that the initial contact angle was $<90°$. No attempt was made to obtain measurements for the final stages of rapid evaporation where the mixed mode of evaporation occurred. It was also noted that the earlier models [117] did not distinguish between the two principal radii of curvature occurring at the contact line: these two radii do not have the same

values. The latter studies therefore extended the model to a two-parameter spherical cap geometry, which was able to explain why the experimentally observed change in contact angle should appear linear in time.

One can describe the state of a liquid drop placed on a smooth solid surface in terms of the radius, height of the drop, and the contact angle, θ. The liquid drop when placed on a smooth solid can have a spherical cap shape, which will be the case in all cases where the drop volume is approximately 10 mL or less. In the case of much larger liquid drops, ellipsoidal shapes may be present, and different geometrical analysis will have to be implemented. On the other hand, in the case of rough surfaces, one may have much difficulty in explaining the dynamic results. However, one may also expect that there will be instances where it is nonspherical. This parameter will need to be determined before any analyses can be carried. Let us assume the case where a spherical cap-shaped drop is present. In the case of a liquid drop that is sufficiently small, ST dominates over gravity. The drop can then be assumed to form a spherical cap shape. A spherical cap shape can be characterized by four parameters: (1) the drop height (h_d), (2) the contact radius (r_b), (3) the radius of the sphere forming the spherical cap (R_s), and (4) the contact angle (θ). By geometry, the relationships between the two radii, the contact angle and the volume of the spherical cap (V_c) are given as [125]

$$r_b = R_s \ \sin(\theta) \tag{1.78}$$

and

$$R_s = \left[\frac{(3\ V_c)}{(p_b)}\right]^{1/3} \tag{1.79}$$

where

$$b = (1 - \cos\theta)^2(2 + \cos\theta) = 2 - 3\cos\theta + \cos 3\theta \tag{1.80}$$

The height of the spherical cap above the supporting solid surface is related to the two radii and the contact angle, θ, by

$$h = R_s(1 - \cos\theta)$$

and

$$h = r_b \ \tan(\theta/2) \tag{1.81}$$

A spherical cap-shaped drop can be characterized by using any two of these four parameters. When the horizontal solid surface is taken into account, the rate of volume decrease by time is given as [8–10]

$$-\left(\frac{\mathrm{d}Vc}{\mathrm{d}t}\right) = \frac{(4pRsD)}{(rL)(cS - c\infty)\, f(\theta)} \tag{1.82}$$

where

t is the time (s)
D is the diffusion coefficient (cm^2/s)
c_S is the concentration of vapor at the sphere surface (at R_s distance) (g/cm^3)
c_∞ is the concentration of the vapor at infinite distance (R_s distance) (g/cm^3)
r_L is the density of the drop substance (g/cm^3)
$f(\theta)$ is a function of contact angle of the spherical cap

In the literature, one finds a few solutions of this relationship [125,126]. Using the analogy between the diffusive flux and electrostatic potential, the exact solution has been derived.

The approximate solution for $f(\theta)$ was given as [125]

$$f(\theta) = \frac{1 - \cos(\theta)}{2} \tag{1.83}$$

while other investigators gave the following relationships [125]:

$$f(\theta) = \frac{\cos(\theta)}{2\ \ln[1 - \cos(\theta)]} \tag{1.84}$$

It was shown that only in some special cases, the magnitude of θ remains constant under evaporation, such was in water–glass system. In this latter case, where contact angle remains constant during evaporation, the following relation can be written:

$$V_c^{2/3} = V_{ct}^{2/3} - (2/3)\ \mathrm{K}f(\theta)t \tag{1.85}$$

Some limited experimental results have been reported that fit this relationship. However, more detailed investigations are needed to understand fully the evaporation phenomena. In only one case [125], has there been reported on the fate of liquid film which remains after most of the liquid has evaporated. It was shown that one could estimate the degree of porosity of solid surfaces from these data. Thus one finds a new method of determination of porosity of solids, without the use of mercury porosimeter [117]. The latter studies are much more accurate, since these were based on measurements of change of weight of drop versus time under evaporation. At this stage in literature, therefore, there is a need for more studies on this dynamic system of liquid drop–solid. Another aspect which also needs more investigations is the features of drying drops placed on solid surfaces, and the Marangoni flow [16].

REFERENCES

1. (a) Bakker, G., Kapillaritat und Uberflachenspannung Handbuch der Eksperimentalphysik, 3d vi, Leipzig, 1928; (b) Freundlich, H., *Colloid and Capillary Chemistry,* Methuen, London, 1926.
2. Adam, N.K., *The Physics and Chemistry of Surfaces*, Clarendon Press, Oxford, 1930.
3. Bancroft, W.D., *Applied Colloid Chemistry,* McGraw-Hill, New York, 1932.
4. Partington, J.R., *An Advanced Treatise of Physical Chemistry*, Vol. II, Longmans, Green, New York, 1951.
5. Harkins, W.D., *The Physical Chemistry of Surface Films,* Reinhold, New York, 1952.
6. Davies, J.T. and Rideal, E.K., *Interfacial Phenomena*, Academic Press, New York, 1963.
7. Defay, R., Prigogine, I., Bellemans, A., and Everett, D.H., *Surface Tension and Adsorption,* Longmans, Green, London, 1966.
8. Gaines, G.L. Jr., *Insoluble Monolayers at Liquid-Gas Interfaces*, Wiley-Interscience, New York, 1966.
9. (a) Matijevic, E., Ed., *Surface and Colloid Science*, Vol. 1–9, Wiley-Interscience, New York, 1969–1976; (b) Holmberg, K., Jonsson, B., Kronberg, B., and Lindman, B., *Surfactants and Polymers in Aqueous Solution*, 2nd edn., John Wiley & Sons, Indianapolis, 2003; (c) Holmberg, K., ed., *Handbook of Applied Surface and Colloid Chemistry*, Vols. 1 and 2, John Wiley & Sons, Indianapolis, 2002; (d) Vadgama, P., ed., *Surfaces and Interfaces for Biomaterials*, Woodhead, 2005; (e) Parsegian, V.A., *Van der Waals Forces*, Cambridge University Press, Cambridge, 2006; (f) Somasundaran, P., ed., *Encyclopedia of Surface and Colloid Science*, 2nd edn., CRC Press, Boca Raton, FL, 2006.
10. Aveyard, R. and Hayden, D.A., *An Introduction to Principles of Surface Chemistry*, Cambridge, London, 1973.
11. Fendler, J.H. and Fendler, E.J., *Catalysis in Micellar and Macromolecular Systems*, Academic Press, New York, 1975.
12. Adamson, A.W., *Physical Chemistry of Surfaces,* 5th edn., Wiley-Interscience, New York, 1990; Faraday Symposia of the Chemical Society, No. 16, *Structure of the Interfacial Region*, Faraday Society, London, 1981.
13. Chattoraj, D.K. and Birdi, K.S., *Adsorption and the Gibbs Surface Excess*, Plenum Press, New York, 1984.
14. Birdi, K.S., *Lipid and Biopolymer Monolayers at Liquid Interfaces*, Plenum Press, New York, 1989; Birdi, K.S., *Self-Assembly Monolayer (SAM) Structures*, Plenum Press, New York, 1999.; (a) Birdi, K.S., *Scanning Probe Microscopes (SPM)*, CRC Press, Boca Raton, FL, 2003; Burg, T.P., Godin, M., Knudsen, S.M., Shen, W., and Manalis, S.R., *Nature*, 446, 1066, 2007.
15. Feder, J., *Fractals: Physics of Solids and Liquids*, Plenum Press, New York; 1988; Avnir, D., ed., *The Fractal Approach to Heterogenous Chemistry*, Wiley, New York, 1989; Birdi, K.S., *Fractals—In Chemistry, Geochemistry and Biophysics*, Plenum Press, New York, 1993.
16. (a) Birdi, K.S., ed., *Handbook of Surface and Colloid Chemistry*, CRC Press, Boca Raton, FL, 1997; (b) Birdi, K.S., ed., *Handbook of Surface & Colloid Chemistry-CD Rom*, CRC Press, Boca Raton, FL, 1997; (c) *Handbook of Surface and Colloid Chemistry*, 2nd edn., 2002.
17. Cosgrove, T., *Colloid Science*, Blackwell, Oxford, 2005.
18. Langmuir, I., *Phys. Rev*., 2, 331, 1913.
19. Parratt, I.G., *Phys. Rev*., 95, 359, 1954.
20. Penfold, J. and Thomas, R.K., *J. Phys. Cond. Matter*, 2, 1369, 1990.
21. Roser, S.J., Felici, R., and Eaglesham, A., *Langmuir*, 10, 3853, 1994.
22. Takahashi, R., *Jpn. J. Appl. Phys*., 2(1), 17, 1983.
23. Vogelsberger, W., Sonnefeld, J., and Rudakoff, G., *Z. Phys. Chemie*, Leipzig, 266, 225, 1985.
24. Butt, H.J., Graf, K., and Kappl, M., *Physics and Chemistry of Interfaces*, J.W.,Wiley, Indianapolis, 2006.
25. Shi, X.D., Brenner, M.P., and Nagel, S.R., *Science*, 265, 219, 1994.
26. Newman, F.H. and Searle, V.H., *The General Properties of Matter*, Butterworths Scientific, London,1957; Green, H.S., *The Molecular Theory of Fluids*, Dover, New York, 1970.
27. Leonardo da Vinci, libri, Histoire des Sciences Mathematiques en Italie, Paris, 3, 54, 1838–1841.
28. Poggendorff, F., *Ann. Phys*., 101, 551, 1857.
29. Gibbs, J.W., *The Collected Works of J.W. Gibbs, Vol. I, Thermodynamics*, Yale University Press, New Haven, CT, 1957.
30. Adam, N.K., *The Physics and Chemistry of Surfaces*, Clarendon Press, Oxford, 1930.

31. Harkins, W.D., *The Physical Chemistry of Surface Films*, Reinhold, New York, 1952.
32. Tadros, T.F., ed., *Colloid Stability*, J.W. Wiley, Indianapolis, 2007.
33. Fu, D., Lu, J.-F., Bao, T.-Z., and Li, Y.-G., *Ind. Eng. Chem. Res*., 39(2), 320, 2000.
34. Hisatomi, M., Abe, M., Yoshino, N., Lee, S., Nagadome, S., and Sugihara, G., *Langmuir*, 16, 1515, 2000.
35. Goodwin, J., *Colloids and Interfaces with Surfactants and Polymers*, John Wiley, Indianapolis, 2004.
36. Rowlinson, J.S. and Widom, B., *Molecular Theory of Capillarity*, Clarendon Press, Oxford, 1982; Abbas, S. and Nordholm, S., *J. Colloid Interface Sci*., 166, 481, 1994.
37. Burshtein, A.A., *Adv. Colloid Interface Sci*., 11, 315, 1979.
38. Young, T., *Trans. Roy. Soc*., 95, 65, 1805.
39. Garflas, F.J., *J. Phys. Chem*., 83, 3126, 1979.
40. (a) Reid, R.C., Prausnitz, J.M., and Poling, B.E., *The Properties of Gases and Liquids*, McGraw-Hill, New York, 1987; (b) Todeschini, R. and Consonni, V., *Handbook of Molecular Descriptors*, Wiley-VCH, 2000.
41. Sugden, S., *J. Chem. Soc*., 125, 32, 1924; Sugden, S., *The Parachor and Valency*, G. Routledge & Sons, London, 1930; Knotts, T.A., Wilding, W.V., Oscarson, J.L., and Rowley, R.L., *J. Chem. Eng. Data*, 46, 158, 2001.
42. Pearson, D. and Robinson, E., *J. Chem. Soc., Faraday Soc*., 736, 1934.
43. Mumford, N. and Philips, L., *J. Am. Chem. Soc*., 52, 5295, 1930.
44. Quale, O.R., *Chem. Rev*., 53, 439, 1953.
45. (a) Tripathi, R., *J. Indian Chem. Soc*., 18, 411, 1941; (b) Saastad, O.W., *J. Chem. Eng. Data*, 43, 617, 1998; (c) Navaza, J.M., *J. Chem. Eng. Data*, 43, 128, 1998; (d) Navaza, J.M., *J. Chem. Eng. Data*, 43, 158, 1998; (e) Jiménez, E., Casas, H., Segade, L., and Franjo, C., *J. Chem. Eng. Data*, 45, 862, 2000; (f) Tsierkezos, N.G., Kelarakis, A.E., and Molinou, I.E., *J. Chem. Eng. Data*, 45, 776, 2000; (g) Tsierkezos, N.G., Kelarakis, A.E., and Palaiologou, M.M., *J. Chem. Eng. Data*, 45, 395, 2000; (h) Lee, J.-W., Park, S.-B., and Lee, H., *J. Chem. Eng. Data*, 45, 166, 2000; (i) Watts, L.A., *Solvent Systems and Experimental Data on Thermal Conductivity and Surface Tension*, G.G. Aseyev. Begell House, New York, 1998; (j) Jimenez, E., *J. Chem. Eng. Data*, 44, 1435, 1999.
46. Stefan, J., *Ann. Phys*., 29, 655, 1886.
47. Waterston, C., *Phil. Mag*., 15, 1, 1858.
48. Eotovos, R., *Ann. Phys*., 27, 448, 1886.
49. Keeney, M. and Heicklen, J., *J. Inorg. Nucl. Chem*., 41, 1755, 1979.
50. Raman, C.V. and Ramdas, L.A., *Phil. Mag*., 3, 220, 1927.
51. McLeod, D.B., *Trans. Faraday Soc*., 19, 8, 1923; (a) Straub, J. and Grigull, U., *Wa.rme- und Stoffu.bertragung*, 13, 241, 1980.
52. Timmerman, J., *Physico-Chemical Constants of Pure Organic Compounds*, Elsevier, New York, 1950. *Selected Properties of Hydrocarbons and Related Compounds*, Vol. 1, API Project 44, Thermodynamics Research Center, A & M University, Texas, 1966.
53. (a) Guggenheim, E.A., *Trans. Faraday Soc*., 41, 150, 1945; (b) Fenelonov, V.B., Kodenyov, G.G., and Kostrovsky, V.G., *J. Phys. Chem. B*, 105, 1050, 2001.
54. Hildebrand, J.H. and Scott, R.L., *Solubility of Nonelectrolytes*, Reinhold, New York, 1950.
55. (a) Somyajulu, G.R., *Int. J. Thermophys*., 9, 559, 1988; (b) Murad, S, *Chem. Eng. Commun*., 24, 353, 1983.
56. Reid, R.C. and Sherwood, T.K., *The Properties of Gases and Liquids—Their Estimation and Correlation*, McGraw-Hill, New York, 1996.
57. Lyman, W.J., Reehl, W.J., and Rosenblatt, D.H., eds., *Handbook of Chemical Property Estimation Methods*, American Chemical Society, Washington, DC, 1990.
58. Le, T.D. and Weers, J.G., *J. Phys. Chem*., 99, 6739, 1995.
59. Wooley, R.J., *Chem. Eng*., March, 109, 1986; Nordholm, S., *Langmuir*, 14, 396, 1998; Felix A. and Carroll, F.A., *Langmuir*, 16, 6689, 2000.
60. (a) Eyring, H. and Jhon, M.S., *Significant Liquid Structures*, John Wiley & Sons, London, 1969; (b) Kimura, H. and Nakano, H.J., *J. Phys. Soc. Jpn*., 54, 1730, 1985; Rey, A.R., *Langmuir*, 16, 845, 2000.
61. Gannon, M.G.J., *Faber Philos. Mag*., A37, 117, 1978.
62. Cini, R., Loglio, G., and Ficalbi, A., *J. Colloid Interface Sci*., 41, 287, 1972.
63. Petty, M.C., *Langmuir–Blodgett Films*, Cambridge University Press, Cambridge, 2004.
64. Koefoed, J. and Villadsen, J.V., *Acta Scand*., 12, 1124, 1958.
65. Hoar, T.P. and Mellord, D.A., *Trans. Faraday Sci*., 53, 315, 1957.
66. Jansen, H.R.S. and Sogor, L., *J. Colloid Interface Sci*., 40, 424, 1972.
67. Jain, D.V.S., Singh, S., and Wadi, R.K., *J. Chem. Soc., Faraday Trans*., 70(I), 961, 1974.
68. (a) Bhatia, A.B., March, N.H., and Sutton, J., *J. Chem. Phys*., 69(5), 2258, 1978; Henderson, J.R., *Mol. Phys*., 39, 709, 1980; (b) Nohira, H., *Langmuir*, 14, 4330, 1998.
69. Carey, B.S., Scriven, L.E., and Davis, H.T., *AICHE J*., 26(5), 705, 1980; Good, R.J. and Buff, F.P., in *The Modern Theory of Capillarity*, Goodrich, F.C. and Tusanov, A.I., eds., Akademie-Verlag, Berlin, Germany, 1981.
70. (a) Sheehan, W.F., *Physical Chemistry*, 2nd edn. Allyn & Bacon, Boston, FL, 1970; (b) Kumar, A., *J. Phys. Chem. B*, 104, 9505, 2000; Kumar, A., *Ind. Eng. Chem. Res*., 38, 4135, 1999.
71. Harkins, R.W. and Wamper, J., *Am. Chem. Soc*., 53, 850, 1931.
72. Lange, N.A. and Forker, G.M., *Handbook of Chemistry*, 10th edn., McGraw-Hill, New York, 1967.
73. Franks, F. and Ives, D.J.C., *Q. Env. Chem., Soc*., 20, 1, 1966.
74. Myers, R.S. and Clever, H.L., *J. Chem. Therm*., 6, 949, 1974.
75. McLure, I.A., Sipowska, J.T., and Pegg, I.L., *J. Chem. Therm*., 14, 733, 1982.

76. (a) McLure, I.A., Soares, V.A.M., Williamson, and Ann, M., *Langmuir*, 9, 2190, 1993; (b) Penas, A., Calvo, E., Pintos, M., Amigo, A., and Bravo, R., *J. Chem. Eng. Data*, 45, 682, 2000; (c) Romero, E., *J. Chem. Eng. Data*, 42, 57, 1997; (d) Navaza, J.M., *J. Chem. Eng. Data*, 41, 806, 1996.
77. McAuliffe, C., *J. Phys. Chem*., 70, 1267, 1966.
78. Choi, D.S., Jhon, M.S., and Eyring, H., *J. Chem. Phys*., 531, 2608, 1970.
79. (a) Tanford, C., *The Hydrophobic Effect*, 2nd edn., John Wiley & Sons, New York, 1980; (b) Yarranton, H.W. and Masliyah, J.H., *J. Phys. Chem*., 100, 1786, 1996.
80. Ben-Naim, A., *Hydrophobic Interactions*, Plenum Press, New York, 1980.
81. Birdi, K.S., The hydrophobic effect, *Trans. Faraday Soc*., 17, 194, 1982.
82. (a) Gurney, R.W., *Ionic Processes in Solution*, Dover, New York, 1953; (b) Frank, H.S. and Evans, M.W., *J. Chem. Phys*., 13, 507, 1945.
83. Langmuir, I., *Third Colloid Symp. Monogr*., 48, 1925.
84. Uhlig, H.H., *J. Phys. Chem*., 41, 1215, 1937.
85. Herman, R.B., *J. Phys. Chem*., 76, 2754, 1972.
86. Ishikawa, S., Hada, S., and Funasaki, N., *J. Phys. Chem*., 99, 11508, 1995.
87. Amidon, G.L., Yalkowsky, H., and Leung, S.J., *Pharm. Sci*., 63, 3225, 1974; Amidon, G.L.L., Yalkowsky, S.H., Anik, S.T., and Valvani, S.C.J., *Phys. Chem*., 79, 2230, 1975.
88. (a) Ramachadran, G.N. and Sasisekharan, V., *Adv. Protein Chem*., 23, 283, 1968; (b) Gao, J. and Jorgensen, W.L., *J. Phys. Chem*., 92, 5813, 1988; (c) Wallqvist, A. and Covell, D.G., *J. Phys. Chem*., 99, 13118, 1995.
89. Gill, S.J., Dee, S.F., Olofsson, G., and Wadso, I., *J. Phys. Chem*., 89, 3758, 1985.
90. Matsuki, H., Hashimoto, S., and Kaneshina, S., *Langmuir*, 10, 1882, 1994.
91. Birdi, K.S., Vu, D.T., and Winter, A., *Proceedings of the 4th European Symposium on Enhanced Oil Recovery*, October 1987, Hamburg, Germany.
92. Fowkes, F.M., *J. Adhes. Sci. Technol*., 1, 7, 1987.
93. Fowkes, F.M., *J. Phys. Chem*., 67, 2538, 1963.
94. Fowkes, F.M., *Ind. Eng. Chem*., 12, 40, 1964; Fowkes, F.M., *J. Phys. Chem*., 84, 510, 1980.
95. Wu, W., Giese, R.F., and van Oss, C.J., *Langmuir*, 11, 379, 1995.
96. Kwok, D.Y., Li, D., and Neumann, A.W., *Langmuir*, 10, 1323, 1994.
97. Aveyard, R. and Briscoe, B.J., *J. Chem. Soc. Faraday Trans*., 68, 478, 1972.
98. Good, R.J., in *Chemistry and Physics of Interfaces*, Ross, S., ed., American Chemical Society, Washington, DC, 1965.
99. Good, R.J., in *Wetting*, van Oss, C.J., ed., Plenum Press, New York, 1992.
100. Bello, J., *J. Theor. Biol*., 68, 139, 1977; Bello, J., *Int. J. Pept. Res*., 12, 38, 1978; Bello, J., *J. Phys. Chem*., 82, 1607, 1978.
101. Herzfeld, H., *Science*, 88, 256, 1992.
102. Cramer, C.J. and Truhlar, D.G., *Science*, 256, 213, 1992.
103. Jorgensen, W.L., Blake, J.F., Madura, J.D., and Wierschke, S.D., *Am. Chem. Soc. Symp. Ser*., 353, 200, 1987.
104. van Gunsteren, W.F. and Berendsen, H.J.C., in *Molecular Dynamics and Protein Structure*, Hermans, J., ed., Polycrystal, Western Springs, IL, 1985.
105. Harte, W.E. and Anderson, E.T., *Proc. Natl. Acad. Sci*., 87, 8864, 1990.
106. Aveyard, R., *J. Colloid Interface Sci*., 52, 621, 1975.
107. Roser, S.J., Felici, R., and Eaglesham, A., *Langmuir*, 10, 3853, 1994.
108. Cosgrove, T., Phipps, J., and Richardson, R.M., *Colloids Surf*., 62, 199, 1992.
109. (a) Mareschat, M., Meyer, M., and Turq, P., *J. Phys. Chem*., 95, 10723, 1991; (b) Willard, N.P., *Langmuir*, 14, 5907, 1998; Kramer E.J., *Macromolecules*, 30, 1906, 1997; Orban, J.M., *Macromolecules*, 29, 7553,1996; Schwarz, S.A., *Macromolecules*, 29, 899, 1996; Menke, T.J., Funke, Z., Maier, R.-D., and Kressler, J., *Macromolecules*, 33, 6120, 2000; Hernáinz, F. and Caro, A., *J. Chem. Eng. Data*, 46, 107, 2001.
110. (a) Angell, C.A., *J. Chem. Educ*., 47, 583, 1970; (b) Angell, C.A., *J. Phys. Chem*., 70, 2793, 1966.
111. Kauzmann, W., *Chem. Rev*., 43, 219, 1948.
112. Hock, R., *Wien Ber*., 108(AII), 1516, 1899.
113. (a) Wu, X.Z., Ocko, B.M., Sirota, C.B., Sinha, S.K., Deutsch, M., Cao, B.H., and Kim, M.W., *Science*, 261, 1018, 1993; (b) Birdi, K.S., *Colloids and Surfaces*, 1997; (c) Back, D.D., *J. Chem. Eng. Data*, 41, 446, 1996.
114. Salajan, M., Glinski, J., Chavepeyer, G., and Platten, J.K., *J. Colloid Interface Sci*., 164, 387, 1994.
115. Motomura, K., in *Capillarity Today, Lecture Notes in Physics*, Vol. 386, Christmann, K., ed., Springer-Verlag, Berlin, 1990.
116. (a) Fragneto, G., Su, T.J., Lu, J.R., Thomas, R.K., and Rennie, A.R. *Phys. Chem. Chem. Phys*., 2, 5214, 2000; (b) Stubenrauch, C., Albouy, P.-A., Klitzing, R.v., and Langevin, D., *Langmuir*, 16, 3206, 2000; (c) Cioci, F., *J. Phys. Chem*., 100, 17400, 1996.
117. Birdi, K.S., Vu, D.T., and Winter, A.L., *J. Phys. Chem*., 93, 3702,1989.
118. Birdi, K.S. and Vu, D.T., *Adhes. Sci. Technol*., 7, 485, 1993.
119. Schwartz, L.W., *Langmuir*, 15(5), 1859, 1999.
120. Chen, L.-J., Yan, W.-J., Hsu, M.,-C., and Tyan, D.-L., *J. Phys. Chem*., 98, 1910, 1994.
121. Picknett, R.G. and Bexon, R., *J. Colloid Interface Sci*., 61(2), 336, 1977.
122. Rowan, S.M., Newton, M.L., and McHale, G., *J. Phys. Chem*., 99, 13268, 1995.
123. McHale, G., Kab, N.A., Newton, M.I., and Rowan, S.M., *J. Colloid Interface Sci*., 186, 453, 1997.
124. Erbil, H.Y., Surface tension of polymers in: *Handbook of Surface and Colloid Chemistry*, Birdi, K.S. ed., CRC Press, Boca Raton, FL, 1997.

125. Erbil, H.Y., *Z Phys. Chem. B*, 102, 9234, 1998; Erbil, H.Y., *J. Adhes. Sci. Technol*., 13, 1405, 1999; Erbil, H.Y., McHale, G., Rowan, S.M., and Newton, M.L., *J. Adhes. Sci. Technol*., 13, 1375, 1999; Erbil, H.Y., McHale, G., Rowan, S.M., and Newlon, M.I., *Langmuir*, 15, 7378, 1999; Erbil, H.Y. and Dogan, M., *Langmuir*, 16, 9267, 2000.
126. Drelich, J., Lakskowski, J.S., and Mittal, K.L., *Apparent and Microscopic Contact Angles*, International Science Publishers, VSP, Leiden, 2002.
127. Preuss, M. and Butt, H.-J., *J. Colloid Interface Sci*., 208, 468, 1998; Sugimoto,Y., Abe, M., Jrlinek, P., Perez, R., Morita, S., and Custance, O., *Nature*, 446&1, 64, 2007.
128. Kamusewitz, H.L., Possart, W., and Paul, D., *Colloids Surface Physiochem. Eng. Aspect*, 156(1), 271, 1999.
129. Extrand, C.W. and Kumagai, Y., *J. Colloid Interface Sci*., 191, 318, 1997.
130. Song, B., Bismarck, A., Tahhan, R., and Springer, J., *J. Colloid Interface Sci*., 197, 68, 1998.